

RECLAMATION

Managing Water in the West

Final Report ST-2019-8284-01

Cracked Embankment Erosion Test



U.S. Department of the Interior
Bureau of Reclamation
Research and Development Office
Science and Technology Program

December 2019

Mission Statements

The Department of the Interior (DOI) conserves and manages the Nation's natural resources and cultural heritage for the benefit and enjoyment of the American people, provides scientific and other information about natural resources and natural hazards to address societal challenges and create opportunities for the American people, and honors the Nation's trust responsibilities or special commitments to American Indians, Alaska Natives, and affiliated island communities to help them prosper.

The mission of the Bureau of Reclamation is to manage, develop, and protect water and related resources in an environmentally and economically sound manner in the interest of the American public.

REPORT DOCUMENTATION PAGE			<i>Form Approved</i> <i>OMB No. 0704-0188</i>	
T1. REPORT DATE December 2019		T2. REPORT TYPE Research		T3. DATES COVERED
T4. TITLE AND SUBTITLE Cracked Embankment Erosion Test			5a. CONTRACT NUMBER RR4888FARD160100010	
			5b. GRANT NUMBER	
			5c. PROGRAM ELEMENT NUMBER 1541 (S&T)	
6. AUTHOR(S) Ted Howard, P.E. Peter Irey, P.E.			5d. PROJECT NUMBER 8284	
			5e. TASK NUMBER	
			5f. WORK UNIT NUMBER 86-68315 and 86-68311	
7. PERFORMING ORGANIZATION NAME(S) AND ADDRESS(ES) Ted Howard and Peter Irey, Geotechnical Engineering, Technical Service Center, Bureau of Reclamation			8. PERFORMING ORGANIZATION REPORT NUMBER	
9. SPONSORING / MONITORING AGENCY NAME(S) AND ADDRESS(ES) Research and Development Office U.S. Department of the Interior, Bureau of Reclamation, PO Box 25007, Denver CO 80225-0007			10. SPONSOR/MONITOR'S ACRONYM(S) R&D: Research and Development Office USACE: U.S. Army Corps of Engineers	
			11. SPONSOR/MONITOR'S REPORT NUMBER(S) ST-2019-8284-01	
12. DISTRIBUTION / AVAILABILITY STATEMENT Final report can be downloaded from Reclamation's website: https://www.usbr.gov/research/				
13. SUPPLEMENTARY NOTES				
14. ABSTRACT (Maximum 200 words) Internal erosion events account for the majority of canal and dam embankment incidents. Index testing has been used to estimate the erodibility of different compacted embankment soils. Index tests include Hole Erosion Tests (HET) and Jet Erosion Tests (JET). These tests provide an indication of different circumstances (such as water content at placement, density, soil type) that impact a soil's erodibility. The results of these tests are often used in risk analyses to help evaluate the likelihood or failure for Reclamation's embankment dams. Recent large-scale erosion tests were completed and compared to HET and JET results. Results from the large-scale tests indicate water content, density, void ratio, and percent saturation have a significant impact on a soil's erodibility. Testing on non-plastic silts and high-plasticity clays revealed surprising results. Under various conditions the erosion rate in the clay was found to be similar to the highly erodible non-plastic silts and under other variations the non-plastic silts eroded as slowly as high-plasticity clays. Results from these tests will be used in the evaluation of embankment erodibility.				
15. SUBJECT TERMS Embankment, Internal Erosion, Scour, Concentrated Leak Erosion, Hydraulic Shear Stress, Gradient				
16. SECURITY CLASSIFICATION OF: U			17. LIMITATION OF ABSTRACT U	18. NUMBER OF PAGES 47
19a. NAME OF RESPONSIBLE PERSON Peter Irey	19b. TELEPHONE NUMBER 303-445-3033			
a. REPORT 1	b. ABSTRACT iii	c. THIS PAGE iii		

S Standard Form 298 (Rev. 8/98)
P Prescribed by ANSI Std. Z39-18

PEER REVIEW DOCUMENTATION

Project and Document Information

Project Name: Cracked Embankment Erosion Test WOID: FA300, OA864

Document Final Report – Cracked Embankment Erosion Test

Document Author(s) Ted Howard, Peter Irey Document Date: December 2019

Peer Reviewer: Dennis Hanneman

Review Certification

Peer Reviewer: I have reviewed the assigned items/sections(s) noted for the above document and believe them to be in accordance with the project requirements, standards of the profession, and Reclamation policy.

Reviewer  Date reviewed 12/30/2019
(Signature)

Acknowledgements

The authors are grateful for the funding provided by the U.S. Army Corps of Engineers (USACE) Risk Management Center and by the Bureau of Reclamation Science and Technology Research Program. The authors also wish to express their gratitude for the valuable contributions, guidance, and thoughtful feedback made by Tony Wahl, Chuck Redlinger, Bobby Rinehart, Dennis Hanneman, Andy Hill, Minal Parekh, Jeanne Major, Bill McCormick, John Batka, Matthew Becker, Tyler Pitcher, Alex Franceski and Kent Scott. Special thanks to the State of Colorado Dam Safety Branch for providing a material source and special thanks to people working in Reclamation's Geotechnical and Hydrologic Laboratories for their expertise and putting up with our disturbances for three years.

Acronyms and Abbreviations

CEET	Cracked Embankment Erosion Test
USACE	U.S. Army Corps of Engineers
RMC	USACE Risk Management Center
Reclamation	Bureau of Reclamation
TSC	Technical Service Center
HET	Hole Erosion Test
JET	Jet Erosion Test
SET	Slot Erosion Test
RCT	Rotating Column Test
τ_c	Hydraulic Shear Stress
C_e	HET Coefficient of Erosion
k_d	JET Coefficient of Erosion
I_{HET}	HET Erosion Rate Index
I_{JET}	JET Erosion Rate Index
i_{avg}	Average Gradient
i_{local}	Local Gradient

Executive Summary

Internal erosion events account for the majority of canal and dam embankment incidents. Index testing has been used to estimate the erodibility of different compacted embankment soils. Index tests include Hole Erosion Tests (HET) and Jet Erosion Tests (JET). These tests provide an indication of different properties and parameters (such as water content at placement, density, soil type) that impact a soil's erodibility. The results of these tests are often used in risk analyses to help evaluate the likelihood of failure for Reclamation's embankment dams and canals.

This report documents results from large-scale erosion tests. These large-scale tests are also compared to HET and JET results. Testing on low-plasticity silts and high-plasticity clays revealed surprising results. Under various conditions, the erosion rate in the clay was found to be similar to the low-plasticity silts and under other variations the low-plasticity silts eroded as slowly as high-plasticity clays.

Results from the large-scale testing found that erosion resistance generally increased with higher water content at the time of compaction. Holding water content constant and increasing the compactive effort generally led to higher erosion resistance. The impact of higher water content at the time of compaction appeared to be very significant as the wet of optimum Bonny Silt performed better than the dry of optimum Highland Clay.

Contents

REPORT DOCUMENTATION PAGE	iii
PEER REVIEW DOCUMENTATION.....	v
Acknowledgements	vii
Acronyms and Abbreviations	vii
Executive Summary	ix
Contents.....	xi
Main Report.....	1
Introduction	1
Literature Review and Background	1
Hole Erosion Test (HET).....	4
Jet Erosion Test (JET)	6
Cracked Embankment Erosion Test	9
Testing Apparatus	9
Testing Materials, Compaction and Quality Control.....	11
Testing Procedures.....	13
Embankment Construction and Crack Formation.....	13
Maintaining constant reservoir and monitoring erosion	22
Monitoring and Post-Processing	23
Results.....	31
Erosion Rates.....	32
Local gradient.....	34
Local Hydraulic Shear Stress	35
Observations.....	35
Verification Testing.....	37
JETs.....	37
Bonny Silt JETs.....	39
Highland Clay JETs	39
HETs	43
Steel Box.....	43
Conclusions	47

Cracked Embankment Erosion Test

***References* 50**

Main Report

Introduction

Reclamation is a water management agency with approximately 600 dams in the 17 western United States and is known for the construction and design of embankment dams, concrete dams, and canals. Reclamation spends significant effort maintaining and monitoring its large inventory of dams and canals. A major concern for embankment dams and canals is internal erosion leading to failure of a facility. Cracking of the embankment (canal or dam) is one of many issues that can lead to internal erosion and was the focus of this research. Cracks can occur due to desiccation, differential settlement, slope instability, deformation from earthquakes, or a host of other causes.

Prior to this research large-scale testing was completed to investigate a filter material's ability to self-heal once cracked [1]. Results from the tests showed sand filters compacted to higher densities can sustain cracks and have difficulty healing. Following the filter research, the team decided to develop a new model to study erosion of embankment core materials (e.g. low-plasticity silt and high-plasticity clay material) through cracks. The testing was designed to allow for erosion to be monitored inside a cracked embankment. These tests are referred to as the Cracked Embankment Erosion Test (CEET).

Currently, Reclamation and USACE utilize research completed using Hole Erosion Test (HET) and Jet Erosion Test (JET) to estimate probability of erosion initiating in different soil types. The HET and JET use smaller controlled lab apparatuses that do not always mimic field conditions. The tests are conducted in a closed, controlled environment using smoothly formed uniform flows. Additionally, the majority of samples tested are compacted at optimum water content near maximum density for standard Proctor compaction.

Due to limitations of the small-scale erodibility tests (JET/HET), the team wanted to investigate the impact large-scale testing, water contents, and densities could have on erosion rates in embankment core material. CEET monitored erosion rates through a 3-foot tall crack in a compacted embankment, similar to the upper reaches of an embankment dam or canal.

Literature Review and Background

Reclamation and USACE rely on risk-informed decision making to assist in prioritizing work and to support justification to reduce or better understand risk. Best practices in dam and levee safety risk analysis have been established by both agencies [2]. Within best practices Reclamation and USACE have developed processes for evaluating internal erosion potential failure modes (PFMs). Internal erosion can occur through an embankment, through, along, or into a foundation,

Cracked Embankment Erosion Test

or along a conduit; and by several different mechanisms (scour, backwards erosion piping, internal migration, suffusion/suffusion). The focus of this research was to evaluate conditions under which erosion of a cracked embankment occurs. Reclamation uses the term 'scour' to describe this process of particle detachment from a crack's sidewalls by flowing water, while USACE uses the term 'concentrated leak erosion.' There are several steps involved in assessing the probability of failure initiated by scour (or concentrated leak erosion) in a crack with the potential failure mode being decomposed into a series of events representing the initiation, continuation, progression and breach phases of the internal erosion process [3] [2]. The CEET research focuses on the 'erosion initiates' event to better understand factors that influence the likelihood of erosion initiating in a crack. The research was not focused on the likelihood of a crack forming, only the likelihood of erosion given the formation of a crack beneath the reservoir surface.

Estimating probability of initiation of erosion in a crack is difficult because it is dependent on many variables such as: material properties (gradation, plasticity, density, water content, void ratio, percent saturation), crack width, crack depth below the water surface, and gradients/hydraulic shear stress of water flowing through the crack. During a risk analysis, most of these variables are unknown; at best, the risk team has a general idea of material properties and estimates a range of crack characteristics and gradients.

For this reason, Reclamation and USACE use research findings that correlate probability of initiation of erosion for different seepage gradients, crack widths, and soil types. Tables are grouped by material type and probability of erosion is estimated based on the crack width and the average hydraulic gradient across the crack through the material of concern (usually the core of a dam). An example is provided in Table 1.

Cracked Embankment Erosion Test

Table 1. – Probability of Initiation in a Crack, for SC Soils with FC>40% or CL-ML soils [2]. Note the tables in Best Practices were adapted from the old “Tool Box” [4].

Estimated Likely Crack Width, W_c (mm)	Average Hydraulic Gradient (i_{ave})					
	0.1	0.25	0.5	1.0	2.0	5.0
1	0.02 (0.05-0.08)	0.1 (0.03-0.4)	0.4 (0.2-0.8)	0.8 (0.3-1.0)	0.9 (0.7-1.0)	0.95 (0.8-1.0)
2	0.1 (0.03-0.4)	0.5 (0.2-0.9)	0.7 (0.3-1.0)	0.9 (0.7-1.0)	0.95 (0.8-1.0)	1.0
5	0.4 (0.2-0.8)	0.8 (0.3-1.0)	0.9 (0.7-1.0)	0.95 (0.8-1.0)	1.0	1.0
10	0.7 (0.3-1.0)	0.9 (0.7-1.0)	0.95 (0.8-1.0)	1.0	1.0	1.0
25	0.9 (0.7-1.0)	0.95 (0.8-1.0)	1.0	1.0	1.0	1.0
50	0.95 (0.8-1.0)	1.0	1.0	1.0	1.0	1.0
75	1.0	1.0	1.0	1.0	1.0	1.0
100	1.0	1.0	1.0	1.0	1.0	1.0

Table 2. – Probability of Initiation in a Crack, for CL-CH Soils or CH soils with LL<65 [2]. Note the tables in Best Practices were adapted from the old “Tool Box” [4].

Estimated Likely Crack Width, W_c (mm)	Average Hydraulic Gradient (i_{ave})					
	0.1	0.25	0.5	1.0	2.0	5.0
1	0.005 (0.002-0.02)	0.02 (0.005-0.08)	0.05 (0.01-0.2)	0.1 (0.03-0.4)	0.2 (0.05-0.5)	0.6 (0.2-0.9)
2	0.01 (0.004-0.04)	0.05 (0.01-0.2)	0.1 (0.03-0.4)	0.3 (0.05-0.6)	0.6 (0.2-0.9)	0.9 (0.7-1.0)
5	0.05 (0.01-0.2)	0.2 (0.05-0.5)	0.3 (0.05-0.6)	0.6 (0.2-0.9)	0.8 (0.3-1.0)	1.0
10	0.1 (0.03-0.4)	0.3 (0.05-0.6)	0.6 (0.2-0.9)	0.9 (0.7-1.0)	0.95 (0.8-1.0)	1.0
25	0.3 (0.05-0.6)	0.6 (0.2-0.9)	0.9 (0.7-1.0)	1.0	1.0	1.0
50	0.6 (0.2-0.9)	0.95 (0.8-1.0)	1.0	1.0	1.0	1.0
75	0.8 (0.3-1.0)	1.0	1.0	1.0	1.0	1.0
100	0.9 (0.7-1.0)	1.0	1.0	1.0	1.0	1.0

The probability of erosion initiating tables were developed through extensive laboratory erosion tests on several different soil types. The majority of this testing was completed by the University of New South Wales [4, 5]. The erosion tests primarily used to develop these tables are the Hole Erosion Test (HET), Slot Erosion Test (SET), Jet Erosion Test (JET), and Rotating Cylinder Test (RCT).

Cracked Embankment Erosion Test

The JET and HET are the more commonly used procedures and are most applicable to the CEET.

Before discussing the CEET apparatus and results it is important to understand the principles and examples that guided the research. HET and JET erosion testing have greatly improved the understanding of different soils' erodibility. A brief description of the HET and JET, pros and cons for each test, and how results from each test compare are included below. The HET and JET have been reviewed/scrutinized by many different parties. The following sections are provided as background information only, for additional details see the associated references [5, 6, 7, 8, 9, 10].

Hole Erosion Test (HET)

The HET measures erodibility of a soil by directing flow through a hole drilled through the center of a specimen. The specimen is prepared in a 4-inch standard Proctor mold, drilled with a 1/4" hole and then loaded into the apparatus for testing. A schematic of the apparatus is shown in Figure 1.

The HET was first developed using constant-flow [6] and further developed into a constant-head test that is more commonly used [5]. Erosion of the hole cannot be directly measured or observed during the test. The flow rate downstream of the specimen is monitored and visually inspected for erosion. When running the test at a constant head, an increase in flow downstream of the specimen is a result of the hole eroding. Post processing at the end of the test relies on the initial hole diameter/volume, final hole diameter/volume, and length of time erosion occurred. Using these measured values, the critical hydraulic shear stress (τ_c) and erosion rate coefficient (C_E) are calculated. The critical hydraulic shear stress refers to hydraulic shear stress at the initiation of erosion. A more thorough review of the HET procedure and post-processing calculations is provided in *Determining Erosion Indices of Cohesive Soils with the Hole Erosion Test and Jet Erosion Test* [7].

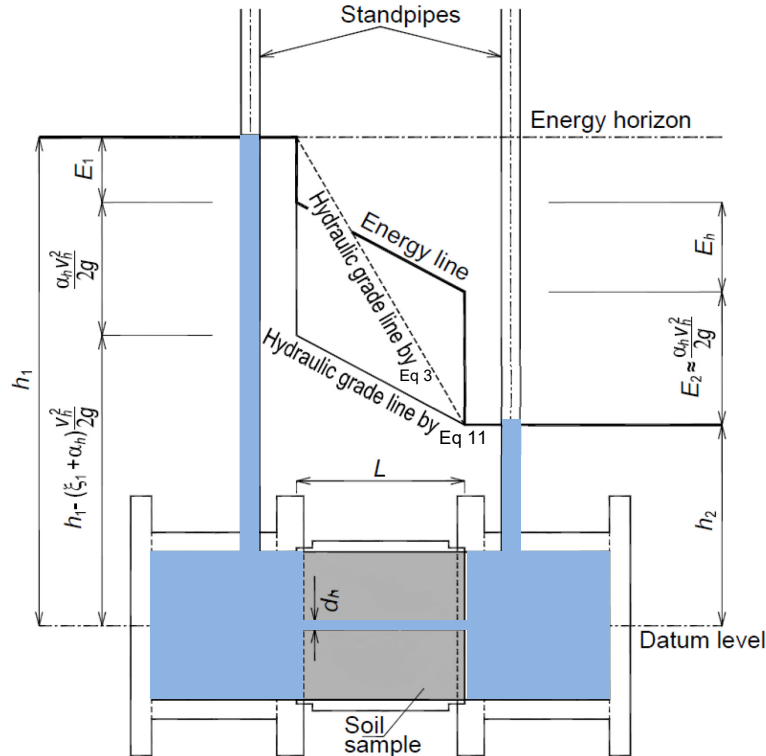


Figure 1. – Schematic of the Hole Erosion Test (from [8]). Hydraulic gradient across the hole was traditionally calculated using equation 3. Equation 11, described by Riha and Jandora [8], updates the equation to account for additional head loss as the flow enters the specimen.

In general, the test is relatively fast, easy to setup/run, and provides repeatable results with respect to relative erodibility of various soil types. Post processing of the results is the most complicated part of the test. There are four main issues affecting the estimation of τ_c and C_E from the HET. The four issues are curve-fitting procedures, variations of the friction factor, determination of final hole diameter, and accounting for entry losses when calculating the gradient across the sample. Three of these issues cause uncertainty in the results and make post processing difficult [7] and are summarized as follows:

- Curve-fitting procedures add complexity to the post processing and are a potential source of error if done incorrectly.
- Assumptions on the linear relationship of friction factors throughout the test can lead to unrealistic calculations of the hole diameter. Unrealistic estimation of the hole diameters has an impact on τ_c and C_E .
- Estimation of the final hole diameter is difficult since the diameter is not always uniform and differing conditions such as sloughing and entry/exit blowout can cause large changes in diameter.

Cracked Embankment Erosion Test

Accounting for entry losses when calculating the average gradient, has the largest impact on the calculation of τ_c [8]. Typically, the gradient is assumed to be linear across the sample, as shown by the dashed hydraulic grade line in Figure 1. Detailed modeling of the specimen was completed using computation fluid dynamic software. The research found that entry losses and the increase in velocity head have a significant impact in calculating τ_c [8].

All four of these issues make estimating of τ_c and C_E difficult and are potential sources of uncertainty in the results. However, HET is still believed to generally model how different soils will behave for scour through a crack or concentrated leak erosion.

Jet Erosion Test (JET)

The JET measures the erodibility of a soil by directing a jet of water at a submerged intact specimen. The specimen is also prepared in a 4-inch standard Proctor mold, submerged in a tank of water, and aligned with a 0.25-inch diameter nozzle placed approximately 6 to 30 nozzle diameters away from the specimen. Note, intact samples may also be used in the HET or JET. A more thorough review of the JET procedure and calculations is provided in *Determining Erosion Indices of Cohesive Soils with the Hole Erosion Test and Jet Erosion Test* [7].

The submerged test procedures were first defined by the U.S. Department of Agriculture, specifically by the Agricultural Research Service Hydraulic Engineering Research Unit [9]. Erosion of the specimen is slightly easier to observe compared to the HET, although cloudy water from the eroding material usually obscures the sample. Erosion rates are monitored by pausing the jet of water using the deflector plate and measuring the depth of the hole using the point gauge. This process is repeated until a predefined time is reached, usually less than 15 minutes for a highly erodible soil or up to 60 minutes for a very erosion-resistant soil. Erosion rates are calculated at the end of the test, results from the JET are reported using k_d the erosion coefficient. Like the HET there are some downfalls to the JET.

Cracked Embankment Erosion Test

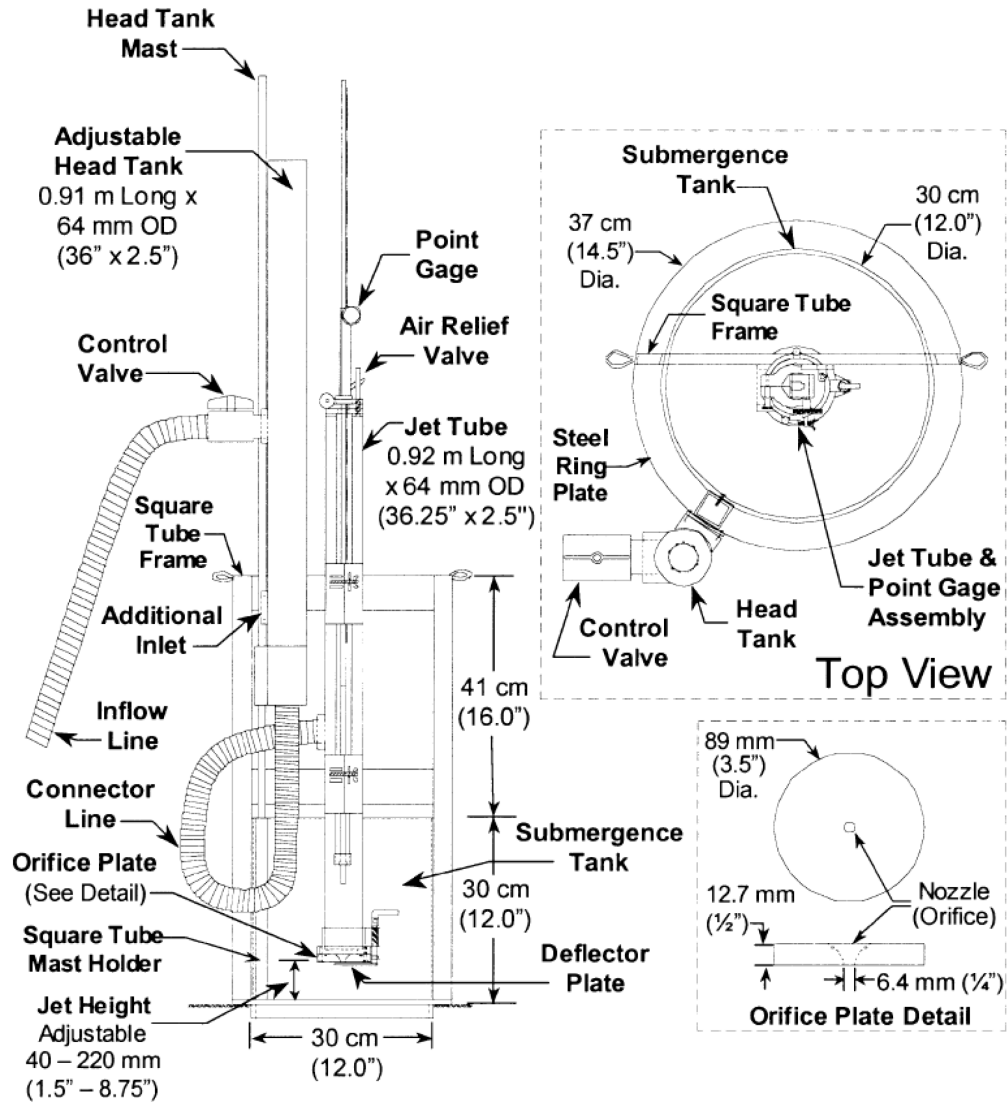


Figure 2. - Schematic of the JET apparatus (from [9])

Cracked Embankment Erosion Test

In general, the JET is also relatively fast, easy to setup/run, and provides repeatable results. Post processing is less of a concern for the JET, but curve fitting is still required to process the results. However, unlike the HET, fewer variables are unknown and there is less uncertainty in the results. One issue with the JET is that the test is often completed on Proctor samples that might not be representative of field conditions. When compacting more than 2 percent wet or dry of optimum, compaction methods used in the standard proctor may not have sufficient energy and may artificially influence the erodibility of the material. Additionally, when compacting soil at optimum water content this may be less of a problem. The JET is more accurately applied to in-situ samples, either on intact samples or using field tests in the field. Another issue with the JET, and arguably the biggest disadvantage of the JET, is that the mechanism that initiates scour better replicates overtopping erosion rather than flow through a crack.

As discussed, both the HET and JET have their disadvantages when estimating erosion rates. In general, the authors believe the HET is more difficult to run and produces less consistent results than the JET. A comparison of the two tests by Reclamation shows why the JET is more consistent [10]. HETs and JETs were completed on the same soil samples and erodibility coefficients and τ_c were compared. Overall, the results from the two tests produce similar erodibility trends, but the HET routinely estimated higher erodibility coefficients and τ_c . The HET also had more difficulties testing soils that were considered very erodible or very erosion resistant. Very erodible to erodible soils often fell apart during the test. An important conclusion from this comparison was the JETs do well over a wider range of soil erodibility and HETs do best over a narrow range of erodibility. Specifically, the HET does best with the intermediate soils, not soils that are very erodible or very resistant [10].

Knowing about the available methods for determining a soil's erodibility, the team was interested if large-scale testing through a cracked embankment would yield similar results. Index tests (HET, JET, SET, RCT, etc.) are great for determining a soil's relative erodibility, but the various test methods do not provide similar absolute values of erodibility parameters. As discussed, these tests are relatively cheap, quick, and repeatable, but the team was interested if flow through a cracked embankment would behave as predicted by large-scale laboratory testing.

Specifically, the team was interested to observe if initiation would be accelerated due to increased local gradients (versus the predicted average gradient), how scour within the crack would initiate (would scour start at the crack entrance, middle or exit), and how the material might self-heal. The apparatus and procedures employed are outlined below. Large-scale tests proved to have many difficulties, most notably quantifying the hydraulic shear stress within the crack. In the end, the results were more qualitative than initially anticipated.

Cracked Embankment Erosion Test

Testing Apparatus

The goal of the large-scale testing was to construct a small embankment (approximately 3 to 5 feet tall) that could allow a crack to be formed and erosion in the crack to be monitored. To do this several other variables needed to be considered before designing the testing apparatus;

- How can the crack be created and allow monitoring of erosion?
- How can a uniform crack be created (consistent from test to test)?
- How to maintain constant head at the crack entrance?
- How to cover a wide range of average gradients (between 0.1 and 1.0 would be ideal)?
- Do cracks extend up to the crest (open channel vs closed conduit)?
- How to reduce the size of the embankment to cut back on labor/time to construct each test?
- How to mimic construction of a large embankment with sheepsfoot/tamping rollers and achieve similar quality control (water control/conditioning, density)?
- How to construct an apparatus that is water tight and can survive multiple tests (force from compaction and repeated saturation)?
- How to contain sediment and minimize damage to equipment such as pumps?

Some of these questions were easier to answer than others. After much consultation with Reclamation's Hydrologic and Geotechnical Laboratory experts, including resident carpenters, the team derived a plan for the CEET apparatus. The apparatus was developed to model the upper three feet of an embankment, canal, or levee with a crack along the outside edge of the embankment. Given the variation in how long erosion may take to initiate, the system for supplying water to the upstream side of the embankment was designed to reach an elevation, then spill into another section and be recirculated. Plan, profile, section, and details of the testing apparatus are included in Appendix A. Some of the details have changed, but Appendix A shows the design concepts used by the carpenters to build the system. The CEET apparatus has three primary components; head box, material box, and tail box. The configuration of all three components is shown in Figure 3.

Cracked Embankment Erosion Test

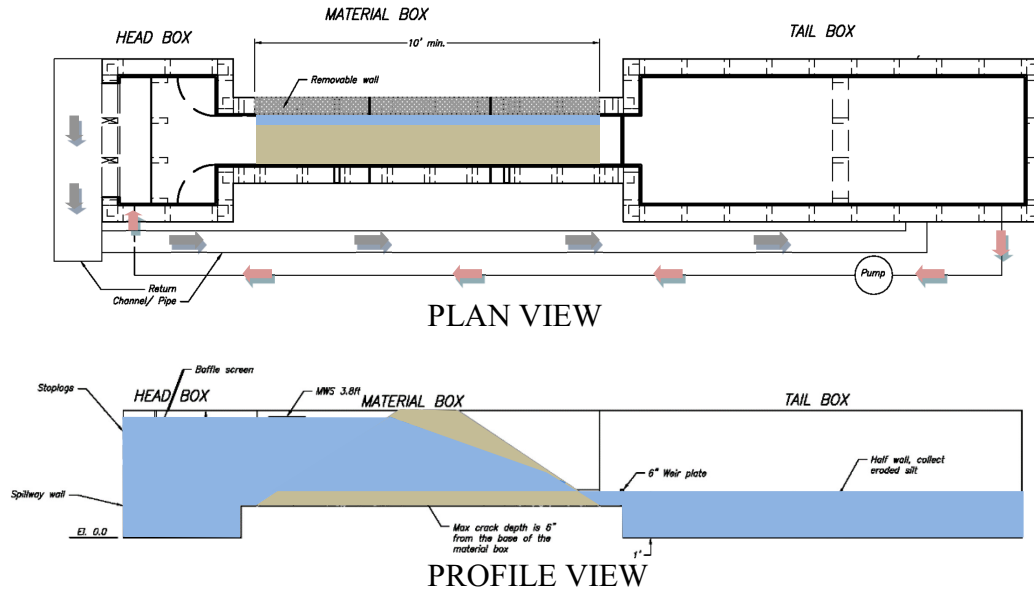


Figure 3. - CEET apparatus plan and profile.

The head box contains the reservoir, which supplies water to the cracked embankment. A spillway was constructed on the upstream end of the head box, and excess water from the pump is sent over the spillway back to the tail box. This allows for a constant reservoir level during each test.

The material box was designed to hold an embankment that was approximately 3.0 feet tall, 12.0 feet long (at the base), and 1.5 feet wide. The material box was designed with a removable wall on one side. Two different removable walls were designed to fit into the same place, see Figure 4.

The first removable wall was designed to protrude into the embankment (i.e. the wall has something attached to it that will be the shape of the flaw). The second removable wall was flat, allowing a crack to form where the protrusion from the first removable wall had been. This second removable wall was transparent, allowing for monitoring of the erosion during the test. Forming the crack in this manner allowed the flaw to have a known approximate initial volume and width, and to be consistent between tests. In Figure 3 the crack is highlighted in blue on the plan view between the brown material and removable water.

Lastly, the tail box is designed to catch sediment and recirculate water back up to the reservoir.

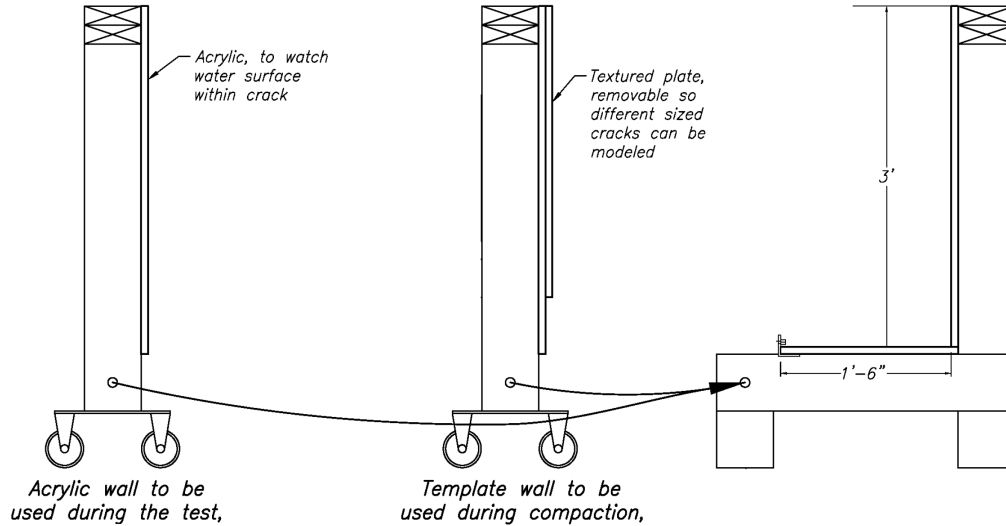


Figure 4. - Section through material box, showing removable wall system.

Testing Materials, Compaction and Quality Control

Two embankment materials were used in the large-scale tests. The embankment materials were selected to represent typical Reclamation embankment cores. The first material was a low-plasticity silt and the second material was a high-plasticity clay.

Silt was acquired from Reclamation's Bonny Dam in eastern Colorado. The material was taken from the original borrow area, located near the dam's right abutment. Physical property testing was completed for the material and is included in Appendix B. The material had an average plasticity index of 6 and has a dual silty-clay classification (CL-ML) per the United Soil Classification System (USCS). The maximum dry density was determined to be 105.2 pounds per cubic foot (pcf) when compacted at 17.0% water content, as determined using American Society for Testing and Material (ASTM) D698. The average gradation has 100% passing the number 4 sieve (no gravel) and 80% passing the number 200 sieve (80% fines). Of the 80% fines, only 10% are classified as clay based on particle size (10 percent passing 2 μ m). Overall, the material was found to be very consistent with only minor changes in plasticity and percent fines. In this report the material is referred to as Bonny Silt.

Clay was acquired from a construction project run by the State of Colorado in Northern Colorado. Physical property testing was completed for the material and is also included in Appendix B. The material had an average plasticity index of 25 and was classified as a Fat Clay to Lean Clay (CH, CL) per USCS. The maximum dry density was determined to be 106.0 pcf when compacted at 20.7% water content, as determined using ASTM D698. The average gradation has 100% passing the 3-inch sieve and 95% passing the number 200 sieve (95%

Cracked Embankment Erosion Test

finer). Of the 95% fines, 48% are classified as clays (48 percent passing 2 μ m) and 53% silt. There were limited amounts of 3-inch material; any 3-inch material encountered during placement of the embankment was removed and no other gravel particles were noted during placement. Overall, the material was found to be very consistent with only minor changes in plasticity and percent fines. In addition to the standard material property tests, a pinhole dispersity test was completed on the clay. Results show that the clay is nondispersive, with a dispersive grade classification of ND2. In this report the material is referred to as Highland Clay.

Stockpile management was a very important part of test preparation. Each embankment constructed in the material box required approximately 15 cubic feet of material. To ensure a consistent water content, approximately 18 cubic feet (or 1,800 pounds) of material was brought into the lab, wetted and thoroughly mixed prior to placement. The researchers tried to only place material once a uniform water content, $\pm 1\%$ of the desired test water content, was reached. Stockpile management was a challenge and this process ensured a more uniform water content.

Compaction was done using a pneumatic, or air powered, backfill tamper (often referred to as a pogo stick) with a custom head attachment, see Figure 5. The pneumatic tamper was manufactured by Sullair [11], weighs 40 pounds, and capable of compacting at 500 blows per minute. A custom head attachment was constructed by Reclamation. The attachment is referred to as the spike-foot attachment, has two-inch long, $\frac{1}{4}$ -inch diameter feet spaced every two inches. This resulted in a localized puncturing-type failure which is more similar to historic sheepsfoot rollers, as opposed to the kneading action generated by the contemporary design of tamping foot rollers. For the wetter material, the local puncture-type failure did result in material being pushed up the sides, and a kneading action was achieved; however, for the drier materials, no kneading action was observed.

The puncturing action replicates the process used in the construction of impervious cores at the large majority of Reclamation and USACE dams.

Cracked Embankment Erosion Test

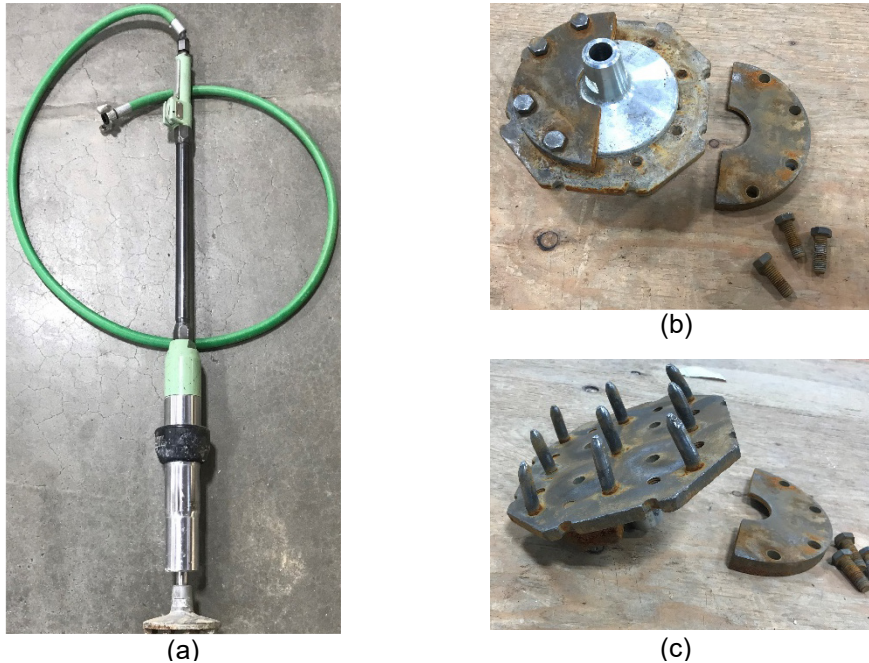


Figure 5. – (a) Sullair backfill tamper with standard flat plate attachment, (b) top of spike-foot attachment that fits over the standard plate, (c) bottom of spike-foot attachment.

Testing Procedures

A total of nine large-scale tests were completed. A standard procedure was developed to improve consistency. Two of the nine tests are considered trials and the results are not compared to the additional seven tests. These two trial tests were used to establish CEET procedures. The general process for each test was to construct the embankment, replace compaction wall with test wall, raise reservoir, maintain reservoir elevation and monitor erosion. The following sections describe these procedures in more detail and describe the critical procedures discovered in the two trial tests.

Embankment Construction and Crack Formation

Each embankment was constructed to be the same size. The embankments were 3 feet tall and 1.5 feet wide. The base of the embankment was ten feet long, both upstream and downstream slopes were at approximately 1.5H:1V. The crest of the embankment was approximately 1 foot long. During compaction the template wall, shown in Figure 4, was locked into place. The embankment shape, upstream to downstream is shown by the dashed outline in Figure 6a.

An important part of each test was ensuring the embankment was well constructed. This meant ensuring consistent density and water content in each embankment. Constant water content was accomplished by preparing large stockpiles ahead of each test, as previously discussed. Density was found to be largely dependent on the amount of confinement provided during compaction.

Cracked Embankment Erosion Test

Confining the embankment during construction was done by constructing the embankment in four levels, as shown in Figure 6 and Figure 7. The process created a stepped embankment. After compaction, forms used to confine the soil were removed and then the slopes were cut down to form typical 1.5 horizontal to 1 vertical slopes.

Density and water content were monitored during each test with sand cone tests. Two sand cone tests were completed on each embankment. Each sand cone test was completed 10 inches below the compacted surface to ensure accurate measurement of density. This was achieved by removing an entire step, completing the sand cone test, and then recompacting the step. Each embankment was constructed with a target water content and the goal to construct the embankment as dense as possible. Percent compaction varied between 90 and over 100%.

During the construction of the embankment a crack was formed into one side of the embankment. To form the crack, a steel plate was mounted to the template wall. Mounting the steel plate to the wall had the additional advantage of making the template wall more rigid while ensuring a uniform crack through the entire embankment. The steel plate protruded into the embankment by 0.375-inches. The crack does not extend down to the base of the model, it stops approximately 6 inches above the base of the embankment to reduce boundary effects at the bottom of the crack. Therefore, the crack consisted of a 0.375-inch thick opening from the crest to within 6 inches of the embankment bases and from the upstream slope to downstream slope. Also, the bottom of the crack is sloped at 1% fall in the downstream direction.

When the template wall was removed from the embankment during trial test 2, portions of the Bonny Silt stuck to the steel, as shown in Figure 8. This caused major disturbance to the crack surface. The disturbed areas were highly erodible and created a non-uniform crack. To overcome this, a thin (0.06 inch) coat of silicone was placed over the entire steel surface. The layer of silicone prevented soil from sticking to the steel. This allowed for a smoother, more uniform crack to be created, as shown in Figure 6b (note the darker vertically oriented streaks in Figure 6b are areas in contact with the steel where silicone was missing). Initially, the team considered lubricating the steel to reduce the likelihood of soil sticking to the steel. However, the lubricant would undoubtedly transfer to the soil and would likely have an impact on the soils' erodibility. For this reason, the silicone was select as the preferred method because it is believed to have had little to no discernible effects on the testing.

After completion of the two trial tests, construction of the embankment and forming the crack became much more uniform. Having a well-established embankment construction procedure was critical to ensure comparison of results between tests.

Cracked Embankment Erosion Test

After compaction of the embankment, the template wall was removed and replaced with the acrylic testing wall. Figure 9 shows the testing apparatus with the acrylic wall installed. The testing wall was constructed from 0.75-inch plexiglass/acrylic. The crack was the 0.375-inch gap between the embankment and acrylic. This gap or crack formed between the wall and embankment is shown in Figure 10. Once the testing wall was in place, the perimeter of the wall was sealed to the apparatus by bolting the removable testing wall to the apparatus. Rubber gaskets and silicone were placed between the removable wall and apparatus to ensure a tight seal. At this point, the embankment was ready to be tested and the reservoir could be filled.

Cracked Embankment Erosion Test

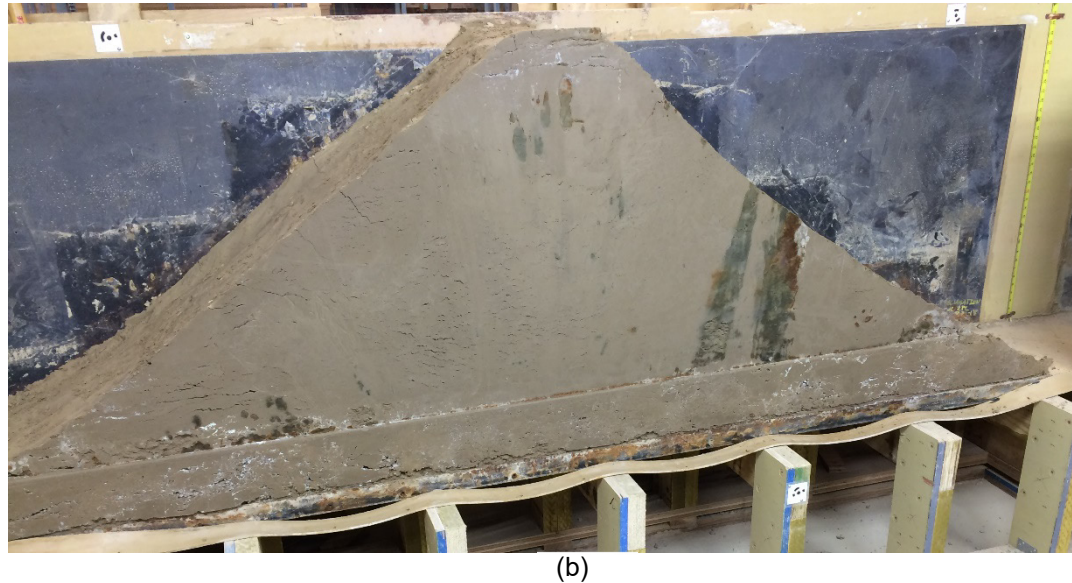
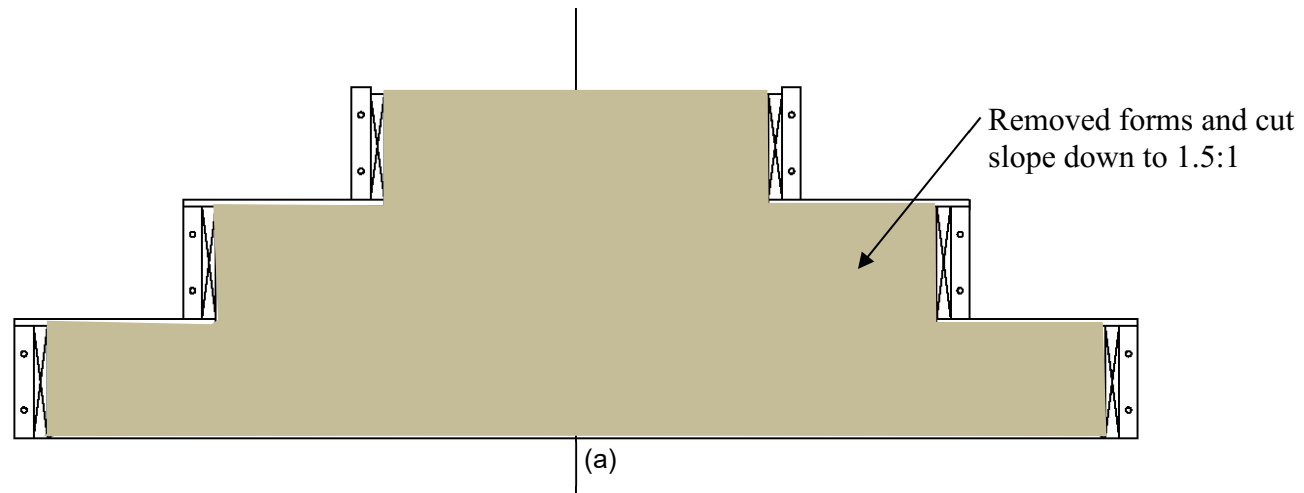


Figure 6. – (a) Schematic of stepped embankment construction, (b) final embankment configuration (picture taken from Test 4). Note, schematic only shows three steps, in actual construction 4 steps were required. Also, figure b shows the embankment after removal of the compaction wall.

Cracked Embankment Erosion Test



(a)



(b)



(c)

Figure 7. – (a) compaction of embankment in step three of four, (b) stepped embankment after removal of forms, (c) embankment after cutting off the steps to create smooth 1.5H:1V slopes. Pictures are taken from Test 2.

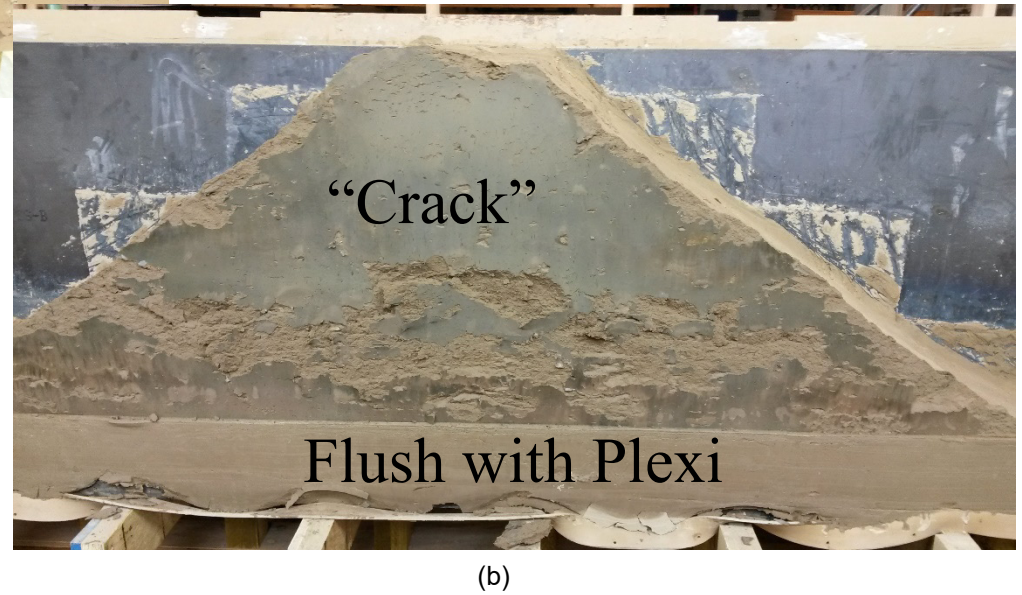


Figure 8. – (a) Image of the template wall showing soil stuck to the steel plate used to form the wall, (b) Embankment showing where soil was removed and how embankment was disturbed. Photos were taken from trial test 2.

Cracked Embankment Erosion Test

Cracked Embankment Erosion Test

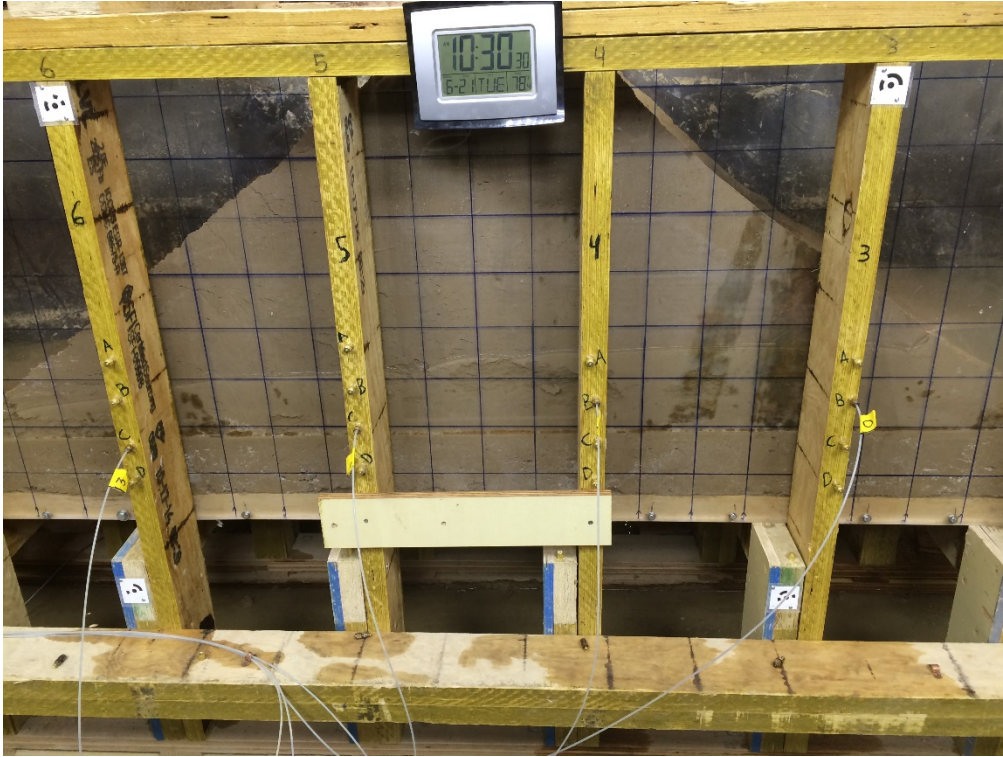


Figure 9. – Apparatus with acrylic glass testing wall installed. Note, grid on acrylic glass is 4-inches by 4-inches.



(a)



(b)

Figure 10. – (a) view of the crack from above the embankment looking down (b) view of the crack from the upstream slope looking towards the reservoir.

Cracked Embankment Erosion Test

Maintaining constant reservoir and monitoring erosion

Constructing the embankment and forming a uniform crack are critical components of each test. Another critical component is operating the test using the same procedures. This includes the operation of the reservoir and average gradients used in each test.

After the acrylic wall is bolted and sealed to the apparatus, the tail box is filled with water. As previously mentioned, the reservoir is supplied by a pump moving water from the downstream tail box to the upstream head box. Figure 11 shows the different components within the head box. The pump has a maximum capacity of 280 gallons per minute (gpm) and the initial 0.375-inch crack only allows 3.5 gpm. The limited flow rate through the crack results in excess water flowing into the spillway and back to the tail box. Reservoir height is controlled by stoplogs in the spillway, adding stoplogs increases the reservoir height and removing logs lowers the reservoir. Directing flow over the spillway allowed the crack width to widen and flow through the crack to increase without a significant change in reservoir elevation. At the beginning of each test when flows through the crack were limited, flow from the pump was throttled using a ball valve. The throttle valve was only fully opened when flow through the crack increased significantly due to the eroding pipe.

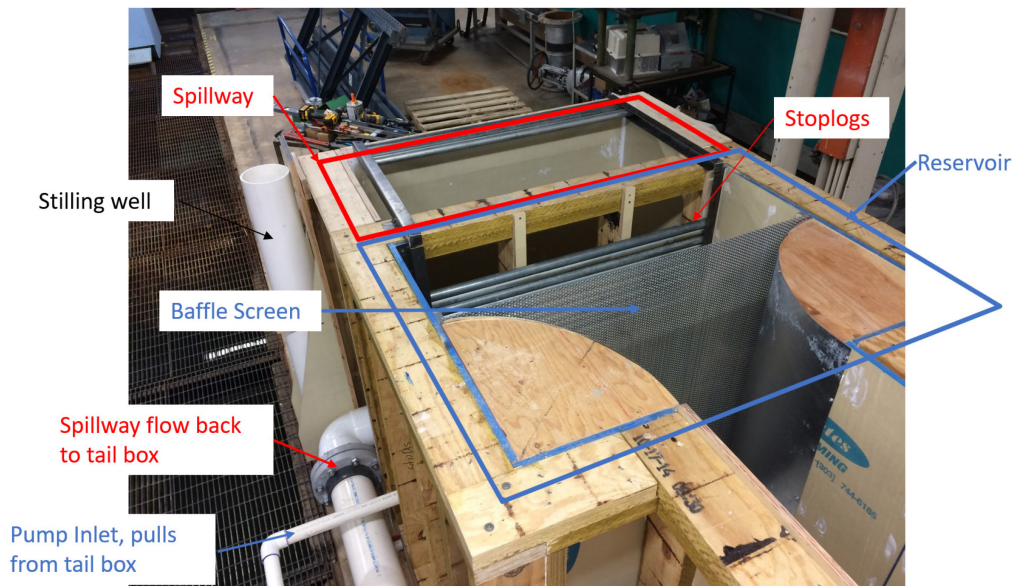


Figure 11. – Image of the head box detailing the different components.

Operation of the reservoir during each test was controlled using the pump and spillway stoplogs. At the beginning of each test the reservoir was filled to 8 inches above the bottom of the crack (15.5 inches above the material box channel). Except for test 3, the reservoir was kept at this elevation for several hours or days depending on the performance of the embankment. During test 3

the reservoir was incrementally raised, changing the reservoir elevation and average gradient across the crack, which impacted the erosion rates. To ensure consistency between tests, all other tests were completed with a reservoir 8 inches above the bottom of the crack. The reservoir was only raised at the end of the test or if no erosion occurred after several days. Test 3 was not used in the estimation of erosion rates.

Raising the reservoir 8 inches above the bottom of the crack resulted in an average gradient of 0.11 across the embankment (length of the bottom of the crack is 6 feet). Assuming the average gradient of 0.11 and crack width of 0.375-inches (~9.5 millimeters) the probability of initiation in a crack can be estimated [2].

Monitoring and Post-Processing

Maintaining a consistent water content, compaction effort, crack width and reservoir head are all critical components to setting up the CEET. The final critical component of the test was processing results from each test and quantifying erosion of the embankment as water flows through the crack. Video cameras and photogrammetry were used to monitor erosion progress throughout the entire test. Velocity and pressure head measurements were taken inside the crack to track changes as erosion progressed. Monitoring of flow rates through the crack and of the reservoir elevation were also done through the entire test.

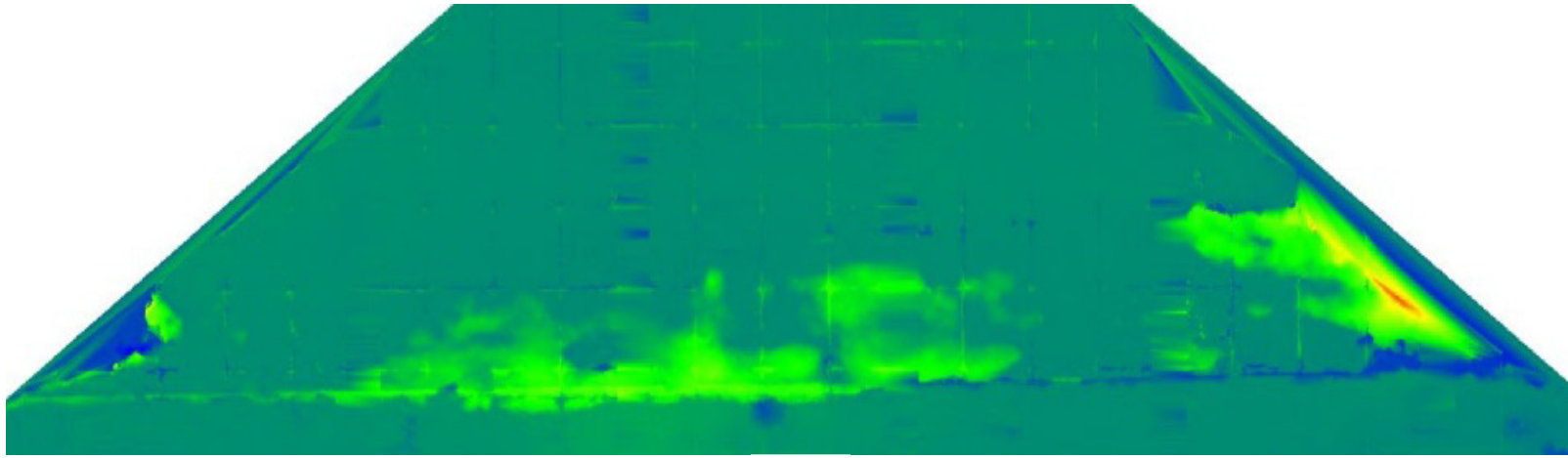
Two cameras were aligned perpendicular to the acrylic testing wall to monitor progression of erosion within the crack and a third camera was placed within the tail box looking upstream towards the embankment. These cameras were left running throughout the entire test to capture progression of erosion. Video from each test has been compiled and reduced; 9-minute summary videos of each test are included in Appendix C. These summary videos are very helpful when comparing erosion progression and rates of embankment erosion. Note the grid sketched on the acrylic glass is 4-inches by 4-inches. The tail water pressure transducer was used to calculate the volume of water passing through the weir.

Photogrammetry was used to quantify the volume of erosion throughout the entire test. The photogrammetric process requires a set of overlapping images to calculate the three-dimensional positions of pixels thereby generating a point cloud and height map of the cross section of the embankment model. For the baseline model, the initial set of photos was taken prior to raising the reservoir. These initial pictures were taken after the acrylic testing wall was put into place. Approximately 40 to 50 high resolution images were captured of the original surface in an overlapping, grid pattern using a full-frame, mirrorless camera on a tripod. Targets were placed around the box to provide scale and a local coordinate system with which to orient the digital model. This allows for accurate comparison of subsequent photogrammetric models. The distances between the targets were measured in the same plane and input into the digital model after calculating the pixel positions. After the baseline set of images were captured, the erosion test was initiated. Once erosion began, the reservoir was lowered, and

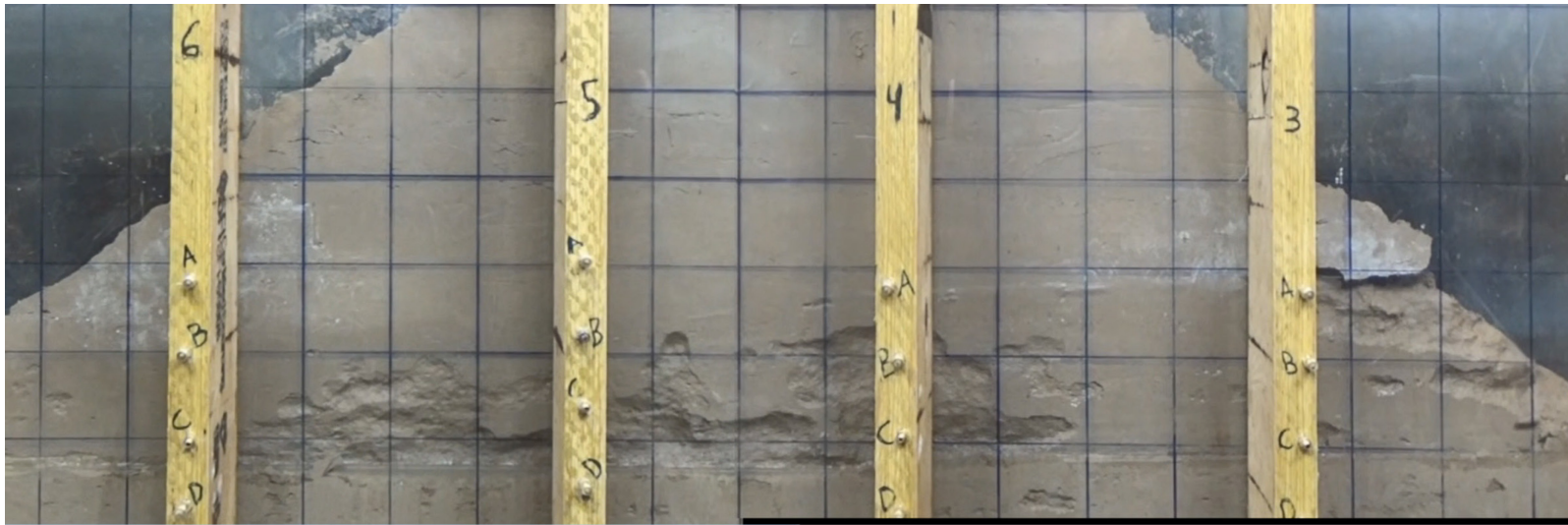
Cracked Embankment Erosion Test

another set of photogrammetric images were captured. This process was continued throughout the erosion test at various points and then the erosion test was conducted to completion, the reservoir emptied, and a final set of images were captured. The number of photogrammetric sets varied per test. The software, Agisoft PhotoScan V1.2.6, was used for the photogrammetric post processing. Since the pictures are taken with the acrylic wall in place the structural members and grid were removed within the software. The model constructed at each interval was then compared to other stages, and the volume change between the two surfaces is estimated using Cloud Compare V2.7. Figure 12 shows the results after processing images of the eroded surface. The results from the photogrammetry were used to estimate erosion rates during each test.

Error and accuracy in the digital modeling was dependent on four factors: 1) measurement of the targets, 2) confidence in the pixel positioning from the photogrammetric processing, 3) scaling the model and 4) alignment of the models during the volume calculation. A common steel tape measure was used to measure the distance between targets and the error within those measurements were taken as 0.8 mm. At about 1-meter offset, the resolution of the images (pixel size) was about 0.16 mm per pixel and the error in the photogrammetric modeling about three-quarters the resolution equaling about 0.13 mm. Of course, areas behind the grid pattern and vertical structural members were interpolated, though the interpolated areas were only about 10% of the total area. The error associated with scaling the model averaged 2.5 mm. Finally, the error in the alignment of the models during the volume calculation was given as the percentage of matching cells and this was about 95%. Volume measurement precision was rounded to the nearest cubic centimeter and the results are estimated with about 10 cubic centimeters of error.



(a)



(b)

Figure 12. – (a) eroded surface constructed from photogrammetry (b) picture of the actual eroded surface. Note the removal of the structural members and the slight grid shown on the photogrammetry surface.

Cracked Embankment Erosion Test

Cracked Embankment Erosion Test

In addition to erosion rate, the team wanted the ability to measure changes in hydraulic shear stress and local gradients within the crack. The average gradient is easily calculated but inside the crack, local changes in velocity head, pressure head and elevation head cause large variations in the local gradient. This head loss may occur over a short distance, causing local gradients within the crack to be much higher than calculated with the average gradient. The Bernoulli equation was used to calculate head loss between two points within the crack.

$$\frac{P_x}{\gamma} + \frac{V_x^2}{2g} + Z_x = \frac{P_y}{\gamma} + \frac{V_y^2}{2g} + Z_y + h_L \quad \text{Equation 1}$$

Where:

- P = pressure (lb/in²)
- γ = weight of water (lb/ft³)
- V = velocity (ft/sec)
- g = acceleration due to gravity (ft/sec²)
- Z = elevation (ft)
- h_L = head loss (ft)

Note, this equation is used to calculate the average gradient as well. The average gradient uses the headwater and tailwater elevations as the difference in total head (the elevation head represents the total head since the top of the water surface has a pressure head of zero, and the water velocity is small enough to be considered negligible) to calculate the average gradient.

This equation can be rearranged to solve for head loss, as described below. Dividing the head loss over the distance the head loss occurs, a local gradient is calculated. Pressure head within the crack was monitored using pressure gauges, velocity within the crack was monitored by adding markers in the reservoir that could be tracked and measured by the video cameras, and elevation head was measured by surveying the apparatus and equipment.

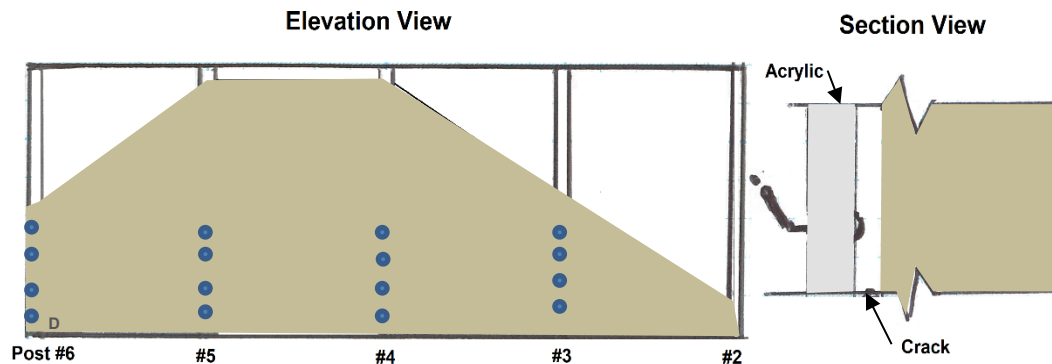


Figure 13. – Schematic used when calculating local gradient between ports. Note, total head within the tube is assumed to be equal to total head in crack.

Cracked Embankment Erosion Test

Solving for head loss:

$$h_L = \Delta P_{x1-x2} + \Delta V_{x1-x2} + \Delta Z_{x1-x2} \quad \text{Equation 2}$$

Where:

$$\Delta P_{4c-5c} = \frac{P_{x1} - P_{x2}}{\gamma} = \text{Change in Pressure Head} \quad \text{Equation 3}$$

$$\Delta V_{4c-5c} = \frac{V_{x1}^2 - V_{x2}^2}{2g} = \text{Change in Velocity Head} \quad \text{Equation 4}$$

$$\Delta Z_{4c-5c} = Z_{x1} - Z_{x2} = \text{Change in Elevation Head} \quad \text{Equation 5}$$

Gradient is then calculated using:

$$i_{local} = \frac{h_L}{L} \quad \text{Equation 6}$$

Where:

L = distance between point 1 and 2

To measure pressure head four pressure transducers were used. The pressure transducers used strain gages embedded into a highly stable silicon wafer. The devices can detect a change in pressure down to 0.08 psi, or a range of accuracy of 0.04 inches of head.

The transducers were connected to ports that penetrated through the acrylic wall into the crack, as shown in Figure 14. The ports on the exterior of the material box were connected to porous stone located inside the crack flush with the acrylic wall. Four ports could be connected at one time. A total of twenty ports were installed, four ports were installed in each post, as shown in Figure 13.

Pressure head was measured at various locations throughout the entire test. Note, pressure sensors were also used to monitor reservoir elevation and tail water elevation. Two additional pressure transducers were continuously monitoring pressure head of the reservoir and tail water downstream of the embankment (upstream of the weir). Note, total head is not directly measured by the instruments. Pressure head in the crack is calculated assuming total head at the port is the same as the total head at the transducer. Pressure head in the crack can then be solved using the following assumptions and equations:

$$h_{e_{inst}} + h_{p_{inst}} = h_{e_{port}} + h_{p_{port}} \quad \text{Equation 7}$$

Where:

Cracked Embankment Erosion Test

he_{inst} is the elevation head of the instrument

hp_{inst} is the pressure head measured by the instrument

he_{port} is the elevation head of the port

hp_{port} is the pressure head at the port

Solving for pressure head at the port:

$$hp_{port} = he_{inst} + hp_{inst} - he_{port} \quad \text{Equation 8}$$

Velocity within the crack was measured by adding hollow glass spheres, HGS, to the reservoir. The HGS are fused borosilicate glass with a hollow non-porous microsphere shape. They have a density of 1.1 grams per cubic centimeter. A mixture of HGS were added to a spray bottle, the spray bottle was inserted in the reservoir upstream of the crack. Squeezing the bottle released a large white cloud of HGS that could be tracked by the video camera. The distance between each post was measured and then an average velocity between each post could be calculated based on the time required for the HGS to travel between posts.

The elevation of the pressure transducers, ports, bottom of the crack, material box floor, and reservoir floor were all surveyed using a level. All components were given an elevation based on the material box floor being at reference elevation 10.0 feet.

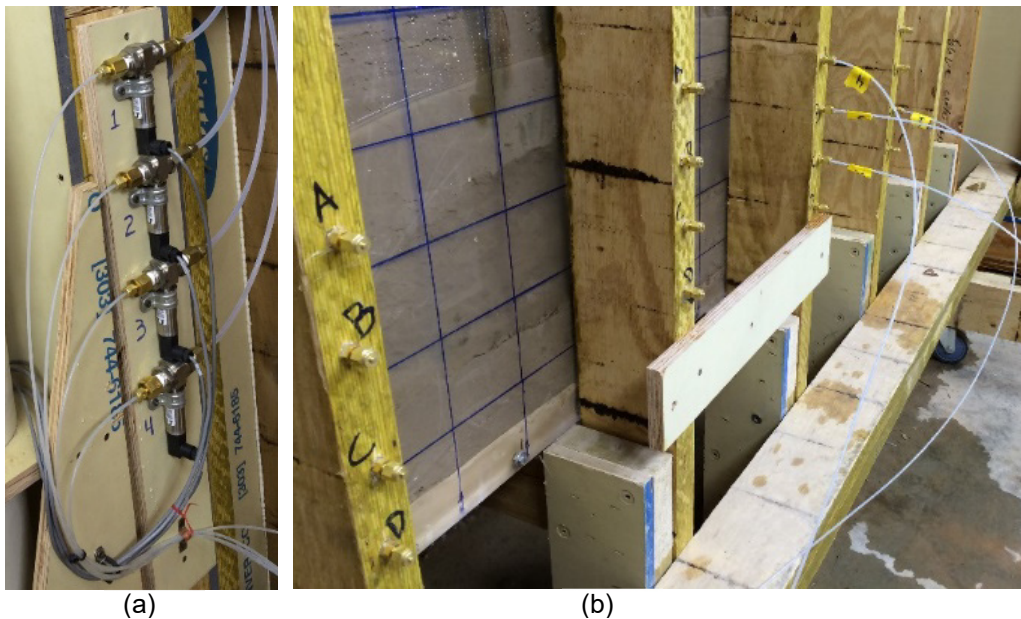


Figure 14. – (a) pressure transducers (b) ports connected to porous stone reading the pressure head within the crack.

Cracked Embankment Erosion Test

Knowing the pressure head, velocity head, and elevation head at several locations within the crack allowed for the calculation of head loss and estimation of the local gradients. As shown in Figure 13, pressure ports were inserted in every post, velocity was measured in between every post, and all critical components were surveyed to measure relative distance and elevation change. This meant an average pressure, velocity and elevation could be measured at each post and the change in these values from post to post could be used to calculate head loss.

Each post was labeled with a number and each port was labeled with a letter, post 4, port C is referred to as 4C. Head loss between each post was computed using Equation 2. For example, pressure transducers would be connected to ports 3C, 4C, 5C, and 6C. While they were connected a velocity test would be completed. Then head loss would be calculated between 3C and 4C, 4C and 5C, and 5C and 6C. This would continue for the entire test. Different ports would be selected depending on the water level within the crack. Calculations of the local gradients were then completed based on the amount of head loss between ports and the distance between each port. Measuring the pressure and velocities within the crack proved significantly more elusive than anticipated, as discussed in the results and uncertainty sections below.

Hydraulic shear stress could also be reported as an average or at local locations within the crack, similar to gradient. Hydraulic shear stresses were calculated using:

$$\tau = \frac{\gamma_w \cdot g \cdot h_L^2 \cdot W}{2 \cdot (h_L + W) \cdot L} \quad \text{Equation 9 [4]}$$

Where:

- τ = hydraulic shear stress (lb/ft²) but often converted to Pascal
- γ_w = weight of water (lb/ft³)
- g = acceleration due to gravity (ft/sec²)
- h_L = head loss (ft)
- W = crack width (ft)
- L = length of crack (ft)

Calculating the initial average hydraulic shear stress, prior to erosion, is straightforward. The average hydraulic shear stress for a 0.375-inch crack with 6-inches of head at the opening is 0.11 pounds per square foot (psf) or 5.5 pascals. For a comparison, the initial shear stress assumed for assessing probability of initiation reported in Table 1 and Table 2 were 0.11 psf (5 pascals) for CL-ML and 0.5 psf (25 pascals) for CL-CH soils [4]. This implies that the hydraulic shear stress may not be high enough to initiate erosion in the Highland clay, hence the low probability of erosion.

Prior to erosion, the crack width is uniform. As the crack width changes the calculation of hydraulic shear stress becomes less straightforward. Calculating the

local hydraulic shear stress requires not only knowing the local change in velocity head, pressure head, and elevation head but also the average crack width. As seen in Figure 12, the crack width can vary greatly between post/ports. Furthermore, the average velocities and pressures measured at the post do not match the velocities and pressures within the eroded areas where the crack is wider. For this reason, calculating local hydraulic shear stress between posts became very difficult, further discussion on the difficulties is provided in the result and uncertainty sections below.

Results

Results are analyzed from six tests; 3 using Bonny Silt and 3 using Highland Clay. Water content and density varied in each test. For both the Bonny Silt and the Highland Clay a test was completed with the material at optimum water content, >2% dry of optimum and >2% wet of optimum. Material type, density, water content, void ratio, and degree of saturation for each test is shown in Table 3.

Table 3. – CEET test overview.

Material Type	Test Number	Dry Weight (pcf)	Percent Compaction	Water Content	Percent from Optimum	Void Ratio	Degree of Saturation
Bonny Silt	4	97.5	93%	19.1%	2.1%	0.71	72%
Bonny Silt	5	106.7	101%	17.0%	0%	0.57	81%
Bonny Silt	6	110.3	105%	13.4%	-3.6%	0.51	70%
Highland Clay	7	108.2	102%	17.1%	-3.6%	0.57	82%
Highland Clay	8	101.6	96%	20.2%	-0.5%	0.67	82%
Highland Clay	9	96.3	91%	23.5%	2.8%	0.76	84%

All of the tests listed in Table 3, were completed with the reservoir 8 inches above the bottom of the crack resulted in an average gradient of 0.11 across the embankment (length of the bottom of the crack is 6 feet). Assuming the average gradient of 0.11 and crack width of 0.375-inches (~9.5 millimeters) the probability of initiation in a crack can be estimated [2]. For Bonny Silt, the probability of erosion initiating is 0.7 (between 0.3 and 1.0) as shown in Table 1; for Highland Clay the probability of erosion initiating is 0.1 (between 0.03 and 0.4) as shown in Table 2. Therefore, it is expected that erosion is likely to occur in the Bonny Silt embankment and unlikely in the Highland Clay under the test conditions. Erosion occurred under an average gradient of 0.11 for all tests conducted on both the Bonny Silt and Highland Clay. After the initial erosion in the Highland Clay tests that were compacted near optimum and above optimum (Tests 8 and 9), it appeared visually that erosion stopped progressing after several

Cracked Embankment Erosion Test

days of constant head. It was necessary to increase the head for erosion to progress to embankment failure.

Erosion Rates

Each of these tests were completed on the same size of embankment using methods previously discussed with a 0.375-inch wide crack and the reservoir 8-inches above the bottom of the crack. The average gradient across the embankment was 0.11 and average hydraulic shear stress was 0.11 psf (5 pa). Note this hydraulic shear stress is calculated at the beginning of the test, prior to any erosion. The amount of erosion varied significantly between tests. Erosion rates were calculated using the volume of eroded material calculated from photogrammetry and the length of time between erosion measurements. Average erosion rates for each test are shown in Table 4 and Figure 15.

Table 4. – CEET erosion rates.

Material Type	Test Number	Water Content	Percent from Optimum	Average Erosion Rate (in ³ /hr)
Bonny Silt	4	19.1%	2.1%	53
Bonny Silt	5	17.0%	0%	245
Bonny Silt	6	13.4%	-3.6%	1,163
Highland Clay	7	17.1%	-3.6%	535
Highland Clay	8	20.2%	-0.5%	17
Highland Clay	9	23.5%	2.8%	5

Cracked Embankment Erosion Test

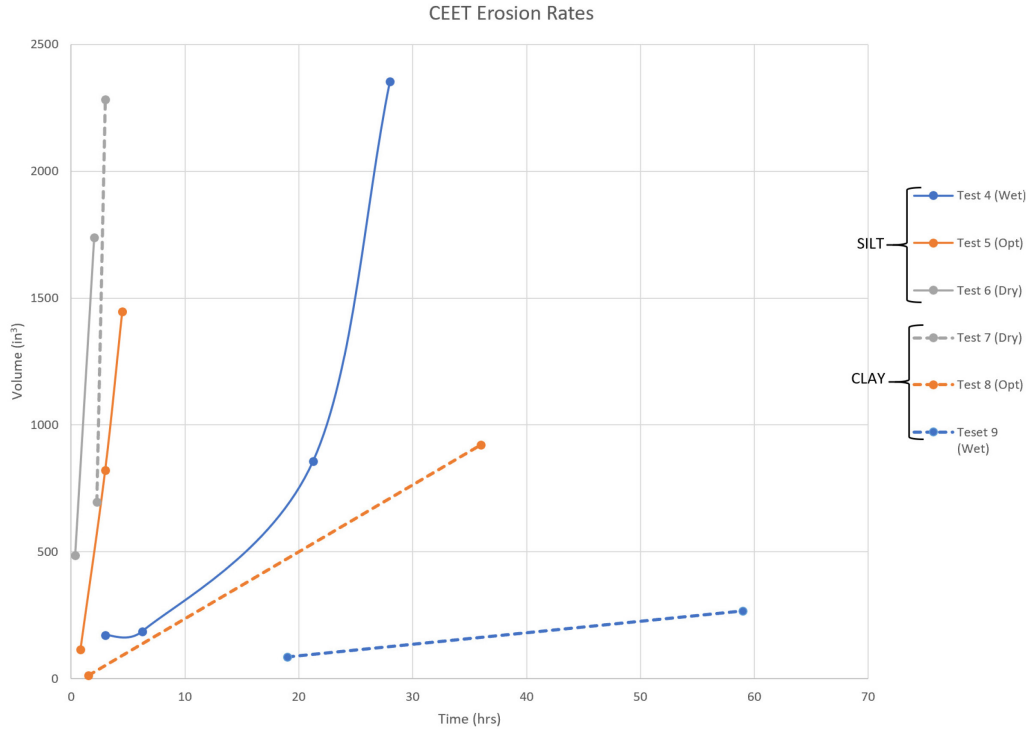


Figure 15. – Erosion rate of cracked embankment erosion tests. Note, final erosion volumes measured in Tests 8 and 9 occurred after gradient was increased.

Overall, Bonny Silt was the more erodible material, especially under optimum and dry of optimum conditions. However, when compacted 3.6% wet of optimum, Bonny Silt erosion rates were similar to the Highland Clay at optimum water content. Overall, Highland Clay was the less erodible. However, at 3.6% dry of optimum, the Highland Clay was as erodible as the Bonny Silt. Erosion rates were easier to quantify in each test using erosion volumes calculated from photogrammetry.

Erosion rates were found to vary significantly between the Bonny Silt and Highland Clay. The trends were similar, indicating that increasing plasticity correlates with increasing erosion resistance. However, as shown on Figure 15 the Bonny Silt compacted near optimum can be grouped with the Bonny Silt compacted dry of optimum and the Highland Clay compacted dry of optimum. The figure also shows that Highland Clay compacted near optimum is generally similar and intermediate between the Bonny Silt compacted wet of optimum and the Highland Clay compacted wet of optimum.

The most telling indicator (independent of material) was found to be water content at the time of compaction. Density (or void ratio) does not appear to be as strong of an indicator. It is reasonable to believe that for a given soil, at a given water content, a higher density sample would perform better than a lower density soil; however, tracking density across material types and different water contents shows an inverse relation to erosion resistance. In other words, the denser soils

Cracked Embankment Erosion Test

(which happened to be drier as well) tended to be less erosion resistant than the looser (and wetter) soils.

Local gradient

The calculations of the local gradients were not the primary focus of this research. The attempts to measure the local gradients were added to the project to evaluate and potentially better define the shear stress occurring during the test on smaller scales than the average gradient.

Calculation of local gradients was difficult to quantify and there are significant uncertainties in the measured/calculated values. There were three components measured in each test; pressure head, velocity head, and elevation head. All three are required to calculate local gradients. Elevation was the easiest to compute and there was very little uncertainty with these estimates. Measurements of the pressure and velocity were more elusive.

In tests 4 through 6, the pressure transducers were mounted in an unfavorable location, which resulted in an insufficient amount of head applied to the instruments. In some instances, the instruments were mounted above the port. This caused significant uncertainty in the readings and for this reason pressure head inside the crack could not be calculated for tests 4 through 6.

Adjustments were made to the location of the instruments for tests 7 through 9. The instruments still had difficulty accurately measuring the pressure head within the crack. During each test multiple pressure head recordings were taken and pressure head in the crack was calculated using Equation 8. The pressure head at the ports was often calculated to be negative. Enough negative readings were recorded that even when a positive value was recorded there was little confidence in the reading. The negative reading is likely caused by small air bubbles in the lines or clogged porous stones in the crack. Several attempts were made to overcome the air bubbles and clogged porous stones. It may also be that the pressure measured at the surface of the acrylic glass was not representative of the pressure in the crack or at the embankment surface. Regardless, it was found the pressure data was unreliable in all the tests.

Velocity measurements were also difficult to obtain. Clouds of HGSs were often too difficult to track. Sometimes this was caused by the transparency of the cloud and other times this was caused by the size of the cloud. It was very difficult to select a common point in the cloud and accurately estimate the arrival and departure time of the cloud. Video was captured at 30 frames per second and often the difference between a few frames per second results in a significant change in velocity.

Due to a lack of confidence in the pressure and velocity readings; results for head loss and local gradients were not included in this report. However, local gradients within a crack are worth considering at least qualitatively. Further discussion

about the qualitative observations of the erosion and local gradients are included below.

Local Hydraulic Shear Stress

Calculations of local hydraulic shear stress have the same sources of uncertainty as measuring crack width. The average crack width is a critical component for estimating the hydraulic shear stress, as seen in Equation 9. Crack widths varied significantly between posts, and while photogrammetry could be used to estimate a depth, the accuracy of the depth due to the variation over a distance causes significant uncertainty. Another factor is that photogrammetry was only available at certain intervals, but often multiple estimations of hydraulic shear stress were attempted between photogrammetry intervals while erosion was occurring.

Observations

Despite the difficulties with quantitative measurements mentioned above, there were many qualitative observations collected during the tests. The different observations were as follows:

- Erosion initiation
- Erosion patterns
- Erosion details

Erosion Initiation

The location of the first eroded particles, and thereby the “epicenter” of erosion tended to be the middle of the embankment for tests 4 through 6.

No direct reason was apparent from the test construction as imperfections were observed elsewhere on the crack face (some staining due to rust, or effervescence from an unknown source) but erosion still started near the middle of the sample. When erosion started in the middle portion of the embankment, the erosion path generally expanded both upstream and downstream from this central point.

During tests 4 through 6, bulging was noticed near the upper middle half of the embankment. The bulging is likely due to the wall deflecting during compaction. However, bulging is less likely to occur below the water surface, where deflection during compaction is less likely. After test 6 the compaction wall was improved and no longer deflected. Erosion in tests 7 through 9 generally occurred throughout the entire crack not just towards the center of the embankment. This may have been due to the lack of crack narrowing or due to the change in material type.

Additionally, it is expected that the embankment would have some movement toward the open gap/crack once the compaction wall was removed. This movement would be greatest where the embankment is highest at the middle of the sample. The amount of displacement due to stress relief was not measured, but a slight narrowing of the gap is possible. Similar deformation behavior would be

Cracked Embankment Erosion Test

expected in a cracked embankment in the field, although the in-situ scenario would have more geometric variability in the crack.

The direction of expansion appeared to depend greatly on other details associated with each test; such as size of eroded pieces, velocity through the crack, and upstream/downstream constrictions.

Erosion Patterns

The observed erosion generally followed a pattern; a piece of the embankment (clod) was removed, and depending on the size of the clod, the velocity of the water, and the geometry of the flaw, the clod may or may not be moved downstream and out of the flaw.

Two other important factors were observed during the tests; the constriction of either the upstream and/or downstream entry/exit point. If the upstream entry was constricted because the entry area did not initially erode, then when a clod fell from the embankment and was removed, the area from which the clod fell increased in cross-sectional area, but did not increase in flow rate, which resulted in a decrease in flow velocity. When this happened consistently (see Test 4), the clods would essentially fall straight down, and the flaw appeared to “migrate” upwards and lateral erosion into the embankment increased, causing localized roof collapse. As the flaw migrated upwards, the downstream end of the flaw would become steeper locally, until the gradient was steep enough to remove the clods. At this point more material would be removed faster and faster until the fallen material was removed and the flow rate through the flaw greatly increased.

When the downstream exit was constricted (Test 8) because it did not initially erode, clods were not able to be removed from the flaw easily, and they were caught at the downstream end. This situation would generally result in the water level rising above the eroded portion of the flaw, and this would increase the frequency of clods falling into the flaw. This also increased the local gradient near the downstream exit, and any constriction was generally eroded out quickly.

Erosion Details Relative to Clod Size

The size of the clods was observed to be critical to erosion rate. The larger the size of the clod, the less likely it was to be transported downstream. It was observed, for both materials, that the water content at the time of compaction was directly correlated to the size of the clods, and the higher the water content, the larger the clod.

Conversely, the tests compacted dry of optimum had very small clod sizes which were transported out of the flaw almost immediately. These tests had the highest erosion rates.

The higher PI material, the Highland Clay, had larger clod sizes at similar water content (compared to optimum) compared to the Bonny Silt.

Verification Testing

JETs

74 JETs were completed on Proctor samples. JETs were completed on both Bonny Silt and Highland Clay, at a variety of water contents and on Proctor samples compacted using standard and modified methods. A list of all the results from each JET is included in Appendix E and a summary of the JET results is included in Table 5 and Table 6. Qualitative descriptions of the soil's erodibility based on k_d , the JET coefficient of erosion, are included in Table 7.

Comparing results between the Bonny Silt and Highland Clay, the overall conclusion is the Bonny Silt is more erodible than the Highland Clay. This is not unexpected based on what is known about each material's physical properties.

Cracked Embankment Erosion Test

Table 5. – Bonny Silt JET results

Compaction Method	Water Content	K _d (ft/hr/psf)		Tc Avg (psf)	# Tests
		Avg (ft/hr/psf)	Standard Deviation		
Standard Proctor	4% Dry	74.7	3.0	0.00027	3
Standard Proctor	2% Dry	7.0	1.3	0.00029	6
Modified Proctor	2% Dry	4.7	1.2	0.00039	9
Standard Proctor	Optimum	7.5	3.1	0.011	9
Modified Proctor	Optimum	1.2	0.2	0.0032	3
Standard Proctor	2% Wet	8.6	6.5	0.0077	11
Modified Proctor	2% Wet	3.3	0.1	0.00050	3
Standard Proctor	4% Wet	0.60	0.23	0.041	3
Total		10.4	17	0.0090	47

Table 6. – Highland Clay Jet Results

Initial Pressure Head	Water Content	K _d (ft/hr/psf)		Tc Avg (psf)	# Tests
		Avg (ft/hr/psf)	Standard Deviation		
High Head	4% Dry	0.60	0.17	0.074	3
Low Head	4% Dry	1.12	0.25	0.00056	3
High Head	2% Dry	0.12	0.061	0.17	3
Low Head	2% Dry	0.22	0.049	0.013	3
High Head	Optimum	0.010	0.0039	1.0	3
Low Head	Optimum	0.165	0.021	0.016	3
High Head	2% Wet	0.003	0.00094	5.12	3
Low Head	2% Wet	0.244	0.042	0.008	3
High Head	4% Wet	0.002	0.00022	2.0	3
Total		0.28	0.36	0.94	27

Table 7. – Qualitative description of rates of erosion for JETs

K _d (ft/hr/psf)	Description
>10	Extremely Erodible
1 – 10	Very Erodible
0.1 – 1	Moderately Erodible
0.01 – 0.1	Moderately Resistant
0.001 – 0.01	Very Resistant
< 0.001	Extremely Resistant

Bonny Silt JETs

Overall, Bonny Silt can be classified as moderately erodible (at 4% wet of optimum) to extremely erodible (at 4% dry of optimum). This means erodibility spans three orders of magnitude. Samples within 2% of optimum are classified as very erodible. JET results for Bonny Silt are also reported graphically in Figure 16. The plot shows how the data is clustered and/or scattered.

Compaction effort was expected to have an impact on the soil's erodibility. Comparing k_d for standard and modified Proctor samples showed a slight decrease in erodibility with additional compaction effort. Standard Proctor samples were consistently reported as very erodible with k_d near 7. Modified Proctor samples were closer to moderately erodible with k_d closer to 1. Note, there is a wide range in k_d estimates for the standard Proctor optimum tests and 2% wet of optimum. The large range in k_d even with the same compaction method and water content may be attributed to the fact that different operators were used throughout the testing.

The average k_d for all 47 Bonny Silt JETs was 10.4, which would classify the material as extremely erodible. Taking an average k_d is not an accurate estimate of the soil's erodibility. Only 25 percent of the samples have a k_d greater than 10, and the average k_d is skewed by a few samples with k_d greater than 70. Using Figure 16, a majority of tests plot in very erodible and the soil could be best summarized as very erodible.

Comparing JET and large-scale embankment erosion testing there are similar trends. As shown in Table 4, erosion rate results from large scale testing show that Bonny Silt was significantly more erosion resistant at 2.1% wet of optimum. The average erosion rate was 53 in³/hr for the large-scale CEET, whereas, the average erosion rates were 245 and 1,163 in³/hr for optimum and dry of optimum tests, respectively. JET results showed less of a change in erodibility at 2% wet of optimum. However, at 4% wet of optimum JET results showed a significant increase in erosion resistance.

Highland Clay JETs

Overall, Highland Clay can be classified as very resistant (at 0 to 4% wet of optimum) to moderately erodible (at 0 to 4% dry of optimum). Highland Clay erodibility also spans three orders of magnitude. JET results for Highland Clay are reported graphically in Figure 17. The plot shows how the data is clustered and/or scattered.

Highland Clay samples were only prepared using standard Proctor methods. However, some of the Highland Clay JETs were completed using a higher preliminary head and others at a lower preliminary head. The low head tests were all completed using 19.5 inches of head and the high head tests all exceeded 36 inches of head. In some cases, the high head tests started at 168 inches. Low head tests completed on the Highland Clay at optimum and wet of optimum had very little erosion and a significantly higher k_d than those completed at higher

Cracked Embankment Erosion Test

heads. The small amount of erosion that occurred during the low head test may have caused the calculation of erosion rate to be artificially increased. Ignoring the low head optimum and wet of optimum tests, the range in k_d between samples at the same water content was more consistent.

JET and large-scale embankment erosion testing results for Highland Clay were in agreement. As shown in Table 4, erosion rate from large scale testing show that Highland Clay was not susceptible to large amounts of erosion; with the exception of 3.6% dry of optimum, for which the Highland Clay eroded at a much higher rate. Note that this rate was higher than the erosion rate of the Bonny Silt at optimum moisture content.

JETs completed on the Highland Clay showed a similar trend. Highland Clay is classified as very resistant to erosion at optimum and wet of optimum (when ignoring the low head tests). However, at dry of optimum, the k_d significantly increases and the material can be classified as moderately to very erodible. As expected, large-scale testing and JET testing showed Highland Clay is more erosion-resistant than the Bonny Silt, except when Highland Clay is compacted more than 2% dry of optimum.

Regardless of material type JET and large-scale tests show erosion resistance is significantly impacted by the water content at the time of compaction. As previously discussed, water content at the time of compaction appears to be the best indicator of erodibility and being dry or wet of optimum could have a significant effect on erodibility. Density, water content, void ratio and degree of saturation also play a role in erodibility but not as clearly as water content at the time of compaction.

Bonny Silt K_d vs Water Content

Note, Optimum Water Content is 17%

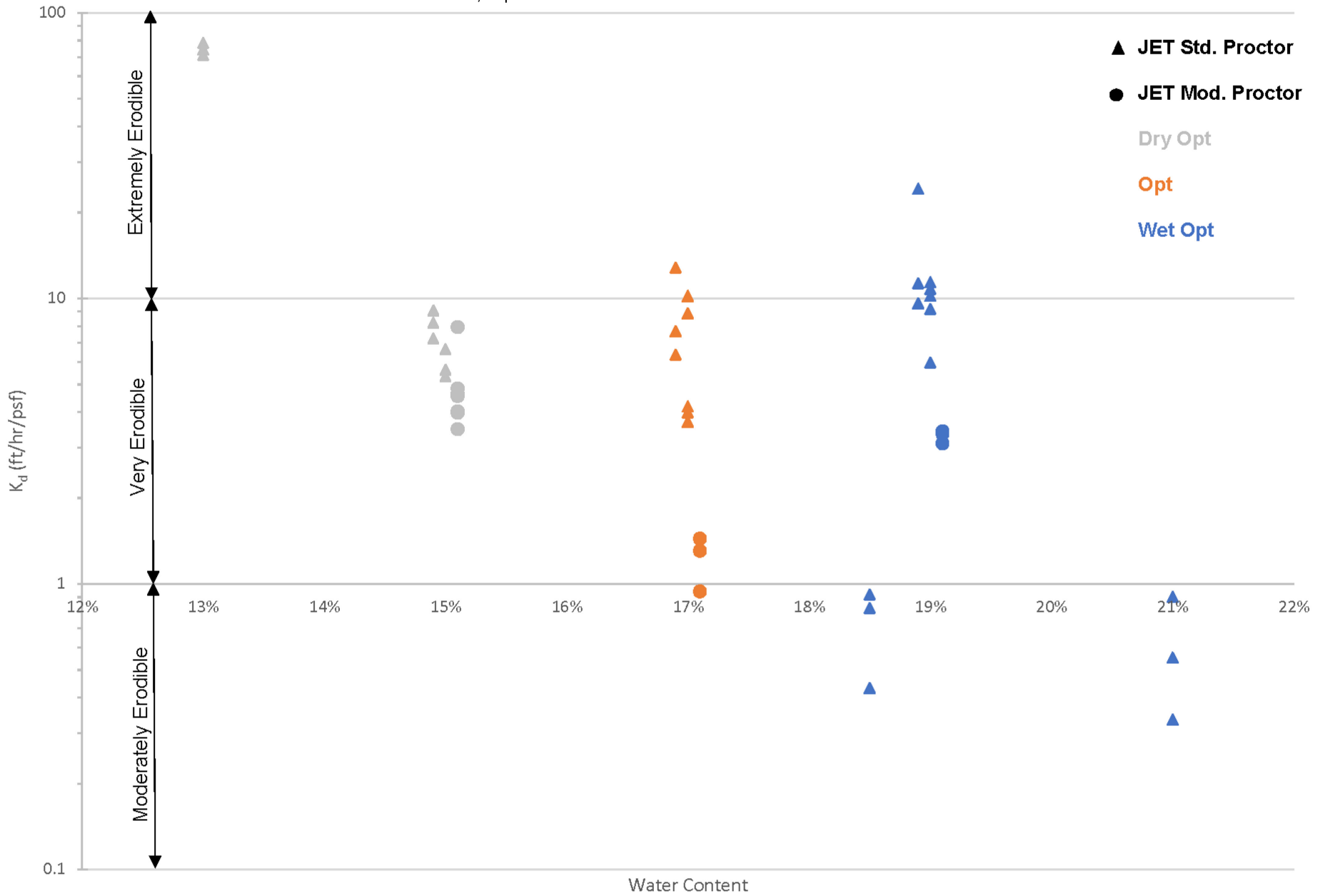


Figure 16. – Bonny Silt JET and HET results.

Cracked Embankment Erosion Test

Highland Clay K_d vs Water Content

Note, Optimum Water Content is 20.7%

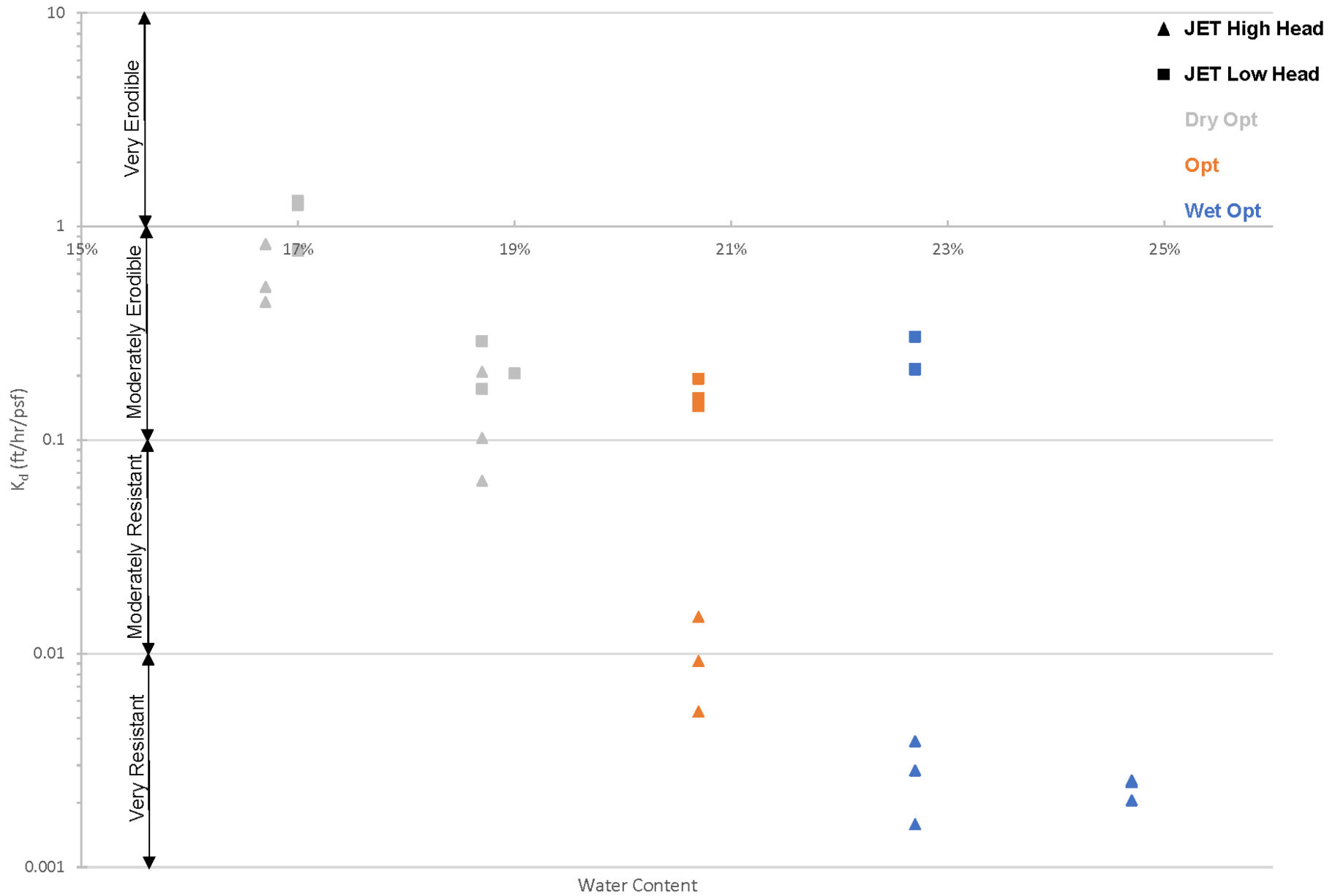


Figure 17. – Highland Clay JET results.

HETs

9 HETs were completed on Proctor samples using Bonny Silt at various water contents. Note, in two of the 7 tests no erosion initiated. Therefore, only 7 tests were used to summarize results. Significantly less HETs were completed due to the difficulties associated with testing very resistant and very erodible materials, difficulty measuring the final hole diameter and overall belief that the JETs were easier to run and provided more consistent results. A list of all the results from each HET is included in Appendix E and a summary of the HET results is included in Table 8.

Unfortunately, HET results obtained for Bonny Silt are considered inaccurate, and therefore, were not plotted or compared to JET or large-scale tests. A review of the calculations revealed an inaccurate measurement of the final hole volume. This inaccurate measurement of the final volume had a significant impact on k_d , τ_c , and I_{HET} calculations.

Table 8. – Bonny Silt HET results

Compaction Method	Water Content	K_d		T_c Avg (psf)	I_{HET}	# Tests
		Avg	Standard Deviation			
Standard Proctor	2% Dry	1.3	1.2	3.7	2.8	2
Standard Proctor	Optimum	1.2	1.1	5.1	5.1	2
Standard Proctor	2% Wet	1.8	1.4	1.7	1.7	3
Total		1.5	1	3.3	3.3	7

Steel Box

9 additional JETS were completed on Highland Clay material. However, instead of compacting the material using standard Proctor methods, the material was compacted in a large steel box using the same pneumatic tamper shown in Figure 5. The steel box was designed to withstand the energy from the pneumatic tamper and to be rotatable with a removable wall so JETs could be completed on the top and side of the compacted material, see Figure 18. The steel box is approximately 18-inches wide by 30-inches long by 18-inches deep.

Cracked Embankment Erosion Test

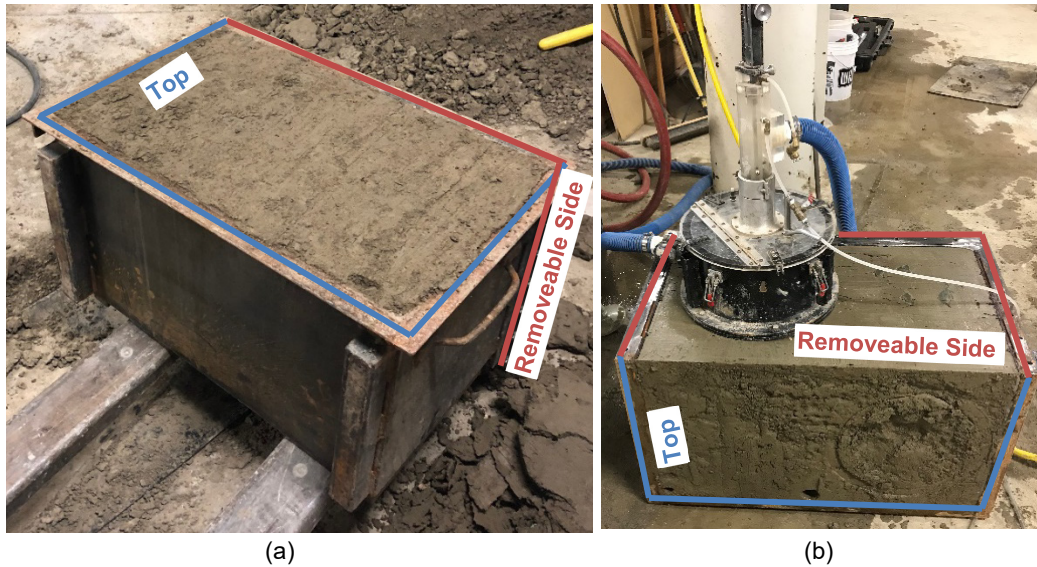


Figure 18. – (a) Steel compaction box shortly after filling. JET was completed on the top before rotating and completing a JET on the side (b).

This method then tested the surface that was compacted, as well as the side perpendicular to the direction of compaction. It was expected that the “side” testing was more similar to the large-scale testing. Only Highland Clay was used in the steel box.

Three different ranges of water contents (optimum, >2% wet, >2% dry) and 3 different compaction techniques (flat plate, spiked plate, and tamper plate) made up all 9 steel box tests. Each compaction technique used the pneumatic tamper with a different plate. The flat plate was approximately 6-inches in diameter with a smooth base (the standard plate noted in Figure 5b), the spike plate is shown in Figure 5b and 5c, the tamper plate was the flat plate with 0.5-inch wide by 0.5-inch thick cubes welded on bottom. Two of three compaction plates (spiked and tamper plates) were designed to simulate compaction techniques found in the field and to provide better compaction than the standard Proctor method; the flat plate was used as a comparison to the standard Proctor compaction method. Results from all 9 steel box tests are included in Table 9 and Figure 19.

Table 9. – Steel box JET results

Compaction Method	Water Content	Dry Density (pcf)	Percent Compaction	Percent Saturation	Void Ratio	JET Top		JET Side	
						k_d (ft/hr/psf)	τ_c (psf)	k_d (ft/hr/psf)	τ_c (psf)
Flat Plate	3% Wet	101.7	96%	89%	0.72	0.18	0.21	0.084	0.13
Flat Plate	Opt	106.1	100%	87%	0.65	0.31	0.20	0.14	0.46
Flat Plate	4% Dry	111.1	105%	79%	0.57	0.016	0.67	0.038	0.86
Spiked Plate	6% Wet	94.6	89%	88%	0.85	0.11	0.27	0.082	0.18
Spiked Plate	Opt	104.0	98%	83%	0.68	0.30	0.39	0.18	0.27
Spiked Plate	4% Dry	105.4	100%	70%	0.66	0.36	0.21	2.6	0.11
Tamper foot	5% Wet	96.9	91%	89%	0.80	0.393	0.11	0.077	0.45
Tamper foot	Opt	109.1	103%	98%	0.60	0.15	0.35	0.18	0.44
Tamper foot	3% Dry	110.5	104%	82%	0.58	0.13	0.36	0.64	0.0053

Cracked Embankment Erosion Test

Highland Clay K_d vs Water Content

Note, Optimum Water Content is 20.7%

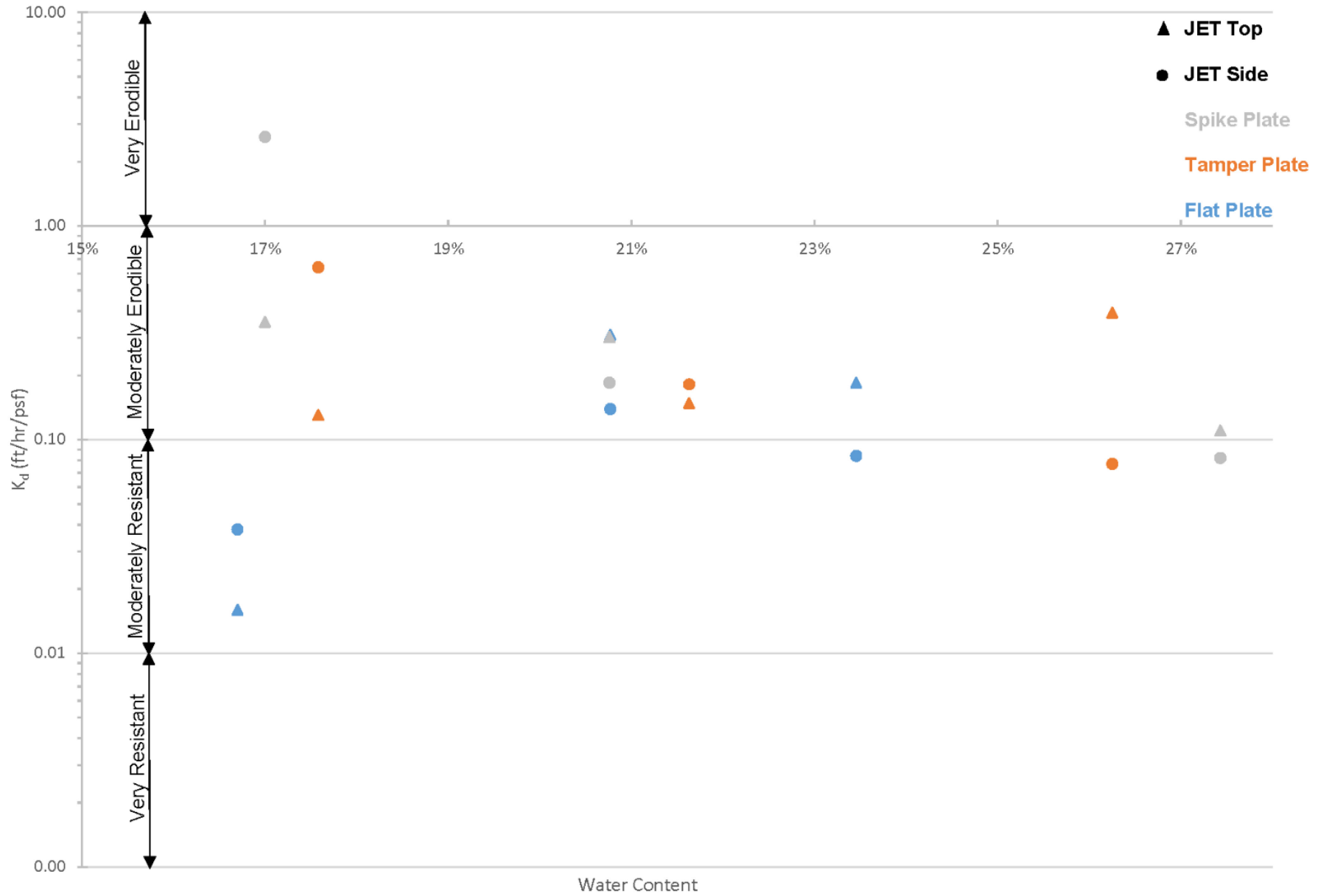


Figure 19. – Steel box JET results.

Overall, JETs completed on the steel box had a relatively narrow range in k_d when compared over a wide range of water contents. Variability in k_d was less for the steel box than for Proctor samples. Less variability in k_d could be due to more energy put into compacting the steel box. Meaning, water content at the time of compaction has less of an impact on soil structure because more energy was used during placement. However, variability for the dry of optimum materials was still high. Dry of optimum flat plate tests had a lower k_d than optimum and wet of optimum tests, this was unexpected and could not be explained. Note, a different operator was used for the dry of optimum flat plate test. Even though the same apparatus and procedures were followed this could be a source of the variability.

After reviewing the results no other trends were identified. The compaction method did not appear to have a major impact on erodibility and neither did direction of the JET. Additional trends may have been identified if additional testing was completed. With only 9 tests to compare the sample size was not large enough to overcome the number of variables.

Conclusions

Large-scale testing on cracked embankments was completed to identify when soil erosion initiates (under what gradients and hydraulic shear stress), how these large-scale tests compare to JET results, and how the initiation of erosion compares to tables included in Reclamations Best Practices [2] that are used to estimate the probability of erosion initiating. Results from the large-scale testing found that erosion resistance generally increased with higher water content at the time of compaction. Holding water content constant and increasing the compactive effort generally led to higher erosion resistance. The impact of higher water content at the time of compaction appeared to be very significant as the wet of optimum Bonny Silt performed better than the dry of optimum Highland Clay.

All large-scale tests started with a crack width of 0.375-inches (~9.5 millimeters) and the reservoir 8 inches over the bottom of the crack. This resulted in an average gradient of 0.11 and average hydraulic shear stress of 0.11 psf (5 pa). Table 1 and Table 2 were used to estimate probability of erosion for the Bonny Silt and Highland Clay material based on an average gradient of 0.1 and a crack width of 10 millimeters. For Bonny Silt, the probability of erosion initiating is 0.7 (between 0.3 and 1.0), for Highland Clay the probability of erosion initiating is 0.1 (between 0.03 and 0.4). The tables estimate Bonny Silt to have a higher probability of erosion higher than the Highland Clay. Erosion initiated in all large-scale tests regardless of material type. However, the rate of erosion and amount of erosion significantly varied based on material type and water content. Highland Clay compacted dry of optimum eroded at a faster rate, similar to the Bonny Silt at optimum or dry of optimum water content. Bonny Silt compacted wet of optimum eroded at a slower rate, similar to the Highland Clay at optimum water content. Table 1 and Table 2, included above and in Reclamation's Best Practices [2], do not account for variations in water content or variation in erosion rates with water content. This research found that erosion may initiate earlier than

Cracked Embankment Erosion Test

the tables estimate, however this does not mean the erosion can progress to failure. Rate of erosion or progression is greatly influenced by the water content at the time of compaction.

The structure of the soil is theorized to be the most critical factor as fine-grained soils compacted wet of optimum are more likely to have the clay particles aligned, and fine-grained soils compacted dry of optimum are more likely to have the clay particles be flocculated/not aligned. This alignment/lack of alignment is believed to influence the size of the clods as particles that are more aligned are more likely to come off in larger chunks (staying together on a macro scale). The particles that are not aligned are likely to be pulled apart easier and not stay together on a macro scale. Similarly, compacting the soil wet of optimum allows for greater kneading of the soil, and more mixing, as the soil is weaker than when it is dry. The kneading effect likely helps the particles align as they are constantly moving around and kneading did not occur with the drier materials.

Additionally, the performance of the embankment during large-scale testing was correlated directly to the size of the clods that were eroded from the exposed face. The larger the size of the clods, the more likely it was that the embankment would self-heal. The size of the clods was directly related to the water content at the time of compaction, and loosely related to the plasticity of the material. Higher water content at the time of compaction led to larger clods, and higher PI material also led to larger clods. These observations from the large-scale tests helped the authors better understand scour processes. Some of the events from a typical Reclamation internal erosion event tree (initiation, self-healing, and progression) were observed throughout the test. When initiation occurs, if self-healing occurred, and how erosion progressed (direction of eroding material progression, roof forming or collapsing) was found to vary between tests and with water content at the time of compaction.

In general, JET results were found to agree with the large-scale tests. At moisture contents greater than 2% wet or dry of optimum a soil's erodibility appears to change significantly. However, there was large scatter in the JET results. This scatter makes it harder to see the effect water content had on the soil's erodibility. Additionally, using low head to conduct JETs on erosion-resistant material can lead to a variety of results. Steel box JET results showed a significant amount of scatter with drier water contents, and less scatter at the higher water contents. The scatter observed in all the verification testing is likely a function of the accuracy of the JET and a function of the poor compaction once water content varies more than 2% away from optimum water content. Accuracy in the testing could have been a function of using multiple operators to obtain the results. However, the accuracy of the JET should not be highly dependent on the operator when the same steps are used.

When using results and trends from JETs the amount of scatter observed in the data should be considered. The erodibility of the soil varied by orders of

Cracked Embankment Erosion Test

magnitude when samples were more than 2% from optimum water content. This should be taken into account when relying on JET results, especially when drawing conclusions from a small sample size. A typical project may only have 3 to 6 JET results to estimate a soil's erodibility.

In general, this research found that compacting embankments more than 3 percent wet of optimum provides greater erosion resistance. Furthermore, compacting embankment material at least 3% wet of optimum would be beneficial around penetrations through an embankment. This may increase construction difficulties and additional consideration should be given to compaction effort/energy. However, there appears to be a significant benefit to compacting material more than 3 percent wet of optimum based on the CEET research.

References

- [1] Large-Scale Filter Performance Test, Report DSO-2014-05, Denver, Colorado: Bureau of Reclamation, July 2014.
- [2] Best Practices in Dam and Levee Safety Risk Analysis, Denver, Colorado: Bureau of Reclamation, U.S. Army Corps of Engineers, 2012.
- [3] B. Doerge, D. Hanneman, T. O'Leary, M. Pabst and K. Richards, Evaluation and Monitoring of Seepage and Internal Erosion, FEMA P-1032, Federal Emergency Management Agency, May 2015.
- [4] R. Fell, M. Foster, J. Cyganiewicz, G. Sills, N. Vroman and R. Davidson, Risk Analysis Methodology - Appendix E, A unified Method for Estimating Probabilities of Failure of Embankment Dams by Internal Erosion and Piping Guidance Document, "Tool Box", University of New South Wales, Bureau of Reclamation, US Army Corps of Engineers, and URS Corporation, 2008.
- [5] C. Wan and R. Fell, "Investigation of rate of erosion of soils in embankment dams," *ASCE Journal of Geotechnical and Geo Environmental Engineering*, vol. 130, no. 4, pp. 373-380, 2004.
- [6] G. Lefebvre, K. Rohan and S. Douville, "Erosivity of Natural Intact Structured Clay," *Canadian Geotechnical Journal*, vol. 22, no. 4, pp. 508-517, 1985.
- [7] T. Wahl, P. Regazzoni and Z. Erdogan, Determining Erosion Indices of Cohesive Soils with the Hole Erosion Test and Jet Erosion Test, Report DSO-08-05, Denver, Colorado: Bureau of Reclamation, Dam Safety Technology Development Program, October 2008.
- [8] J. Riha and J. Jandora, "Pressure Conditions in the Hole Erosion Test," *Canadian Geotechnical Journal*, vol. 52, no. 1, pp. 114-119, 2015.
- [9] G. Hanson and K. Cook, "Apparatus, test procedures, and analytical methods to measure soil erodibility in situ," *Applied Engineering in Agriculture*, vol. 20, no. 4, pp. 455-462, 2004.
- [10] T. Wahl, "A Comparison of the Hole Erosion Test and Jet Erosion Test," in *Joint Federal Interagency Conference on Sedimentation and Hydrologic Modeling*, Las Vegas, 2010.
- [11] "Sullair.com," Sullair, December 2019. [Online]. Available: <https://america.sullair.com/en/products/backfill-tamper#tabs>.
- [12] S. Lim, Experimental Investigation of Erosion in Variably Saturated Clay Soils, A thesis submitted in partial fulfillment of the requirements for the degree of Doctor of Philosophy, School of Civil and Environmental Engineering, The University of New South Wales, 2006.

Appendices

Appendix A	CEET Apparatus Drawings
Appendix B	Material Properties
Appendix C	Summary of Tests 3 through 9
Appendix D	Video Summary of Each Large-Scale Test (Digital Files)
Appendix E	JET and HET results

Appendix A

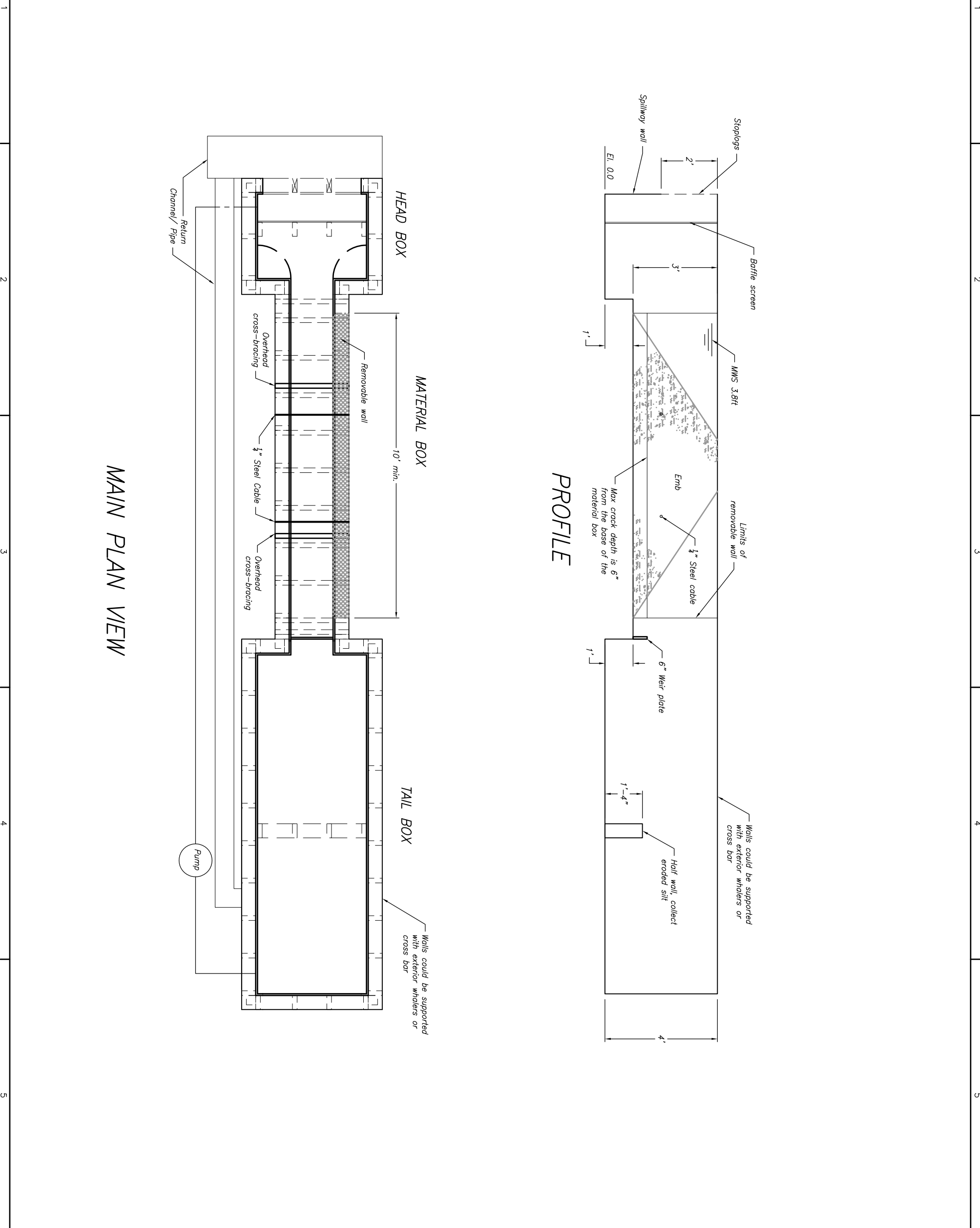
CEET Apparatus Drawings

A

B

C

D



MAIN PLAN VIEW

PROFILE

P. IRBY	DESIGNED
P. IRBY	DRAWN
OSAMA	CHECKED
T. HOWARD	TECH. SUPPORT
T. WAH	ADMIN. APPROVAL
DENVER, CO	2014-12-03

OVERALL PLAN AND
PROFILE

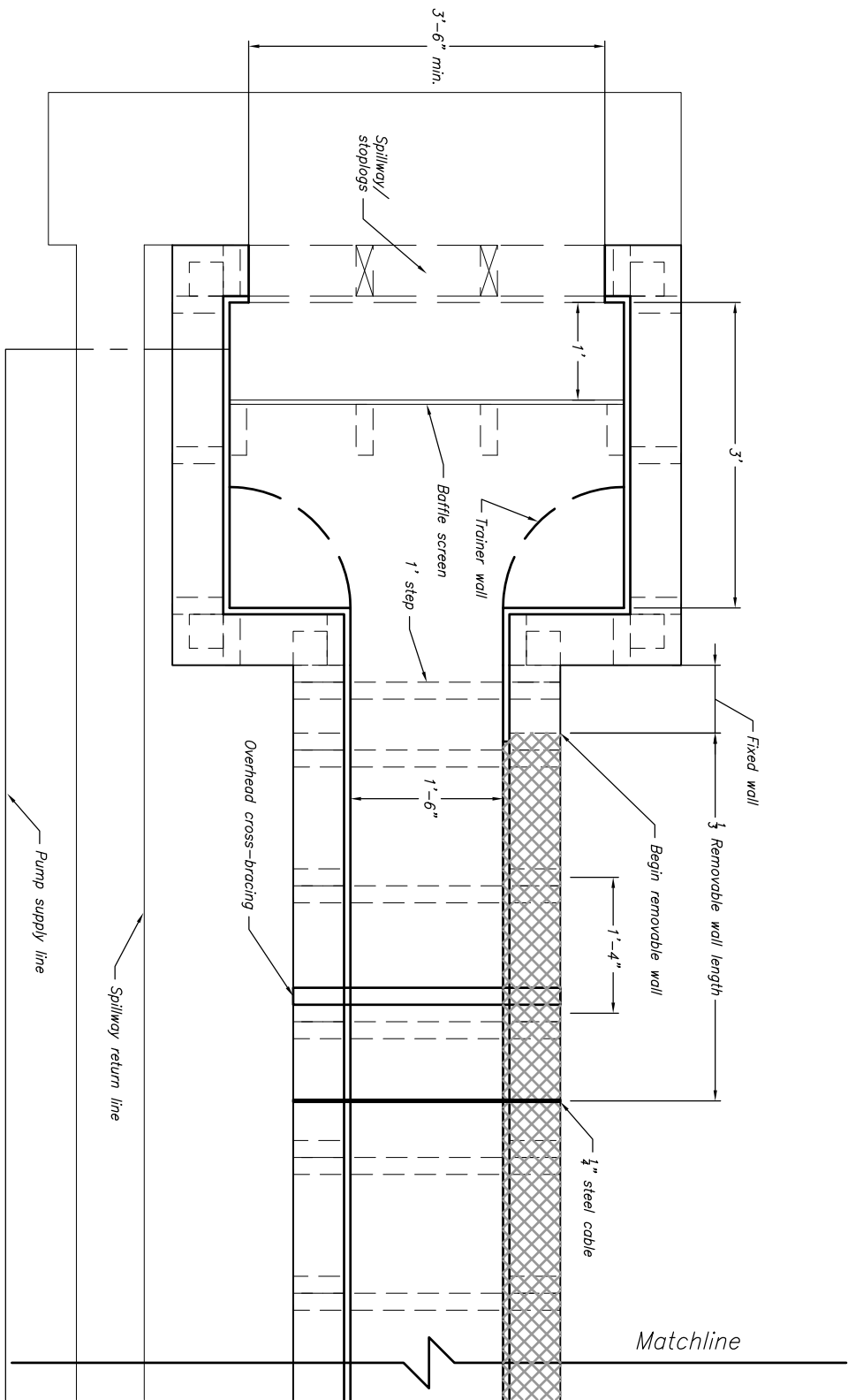
CEET-BOX-1
SHEET 1 OF 4

ALWAYS THINK SAFETY

U.S. DEPARTMENT OF THE INTERIOR
BUREAU OF RECLAMATION

EROSION RESEARCH
TECHNICAL SERVICES CENTER, COLORADO

**CREST EMBANKMENT EROSION TEST
PROPOSED MODEL**



PLAN VIEW PART 1



- NOTES**
1. Carpenters to determine head box and tail box interior dimensions based on minimum spillway widths.

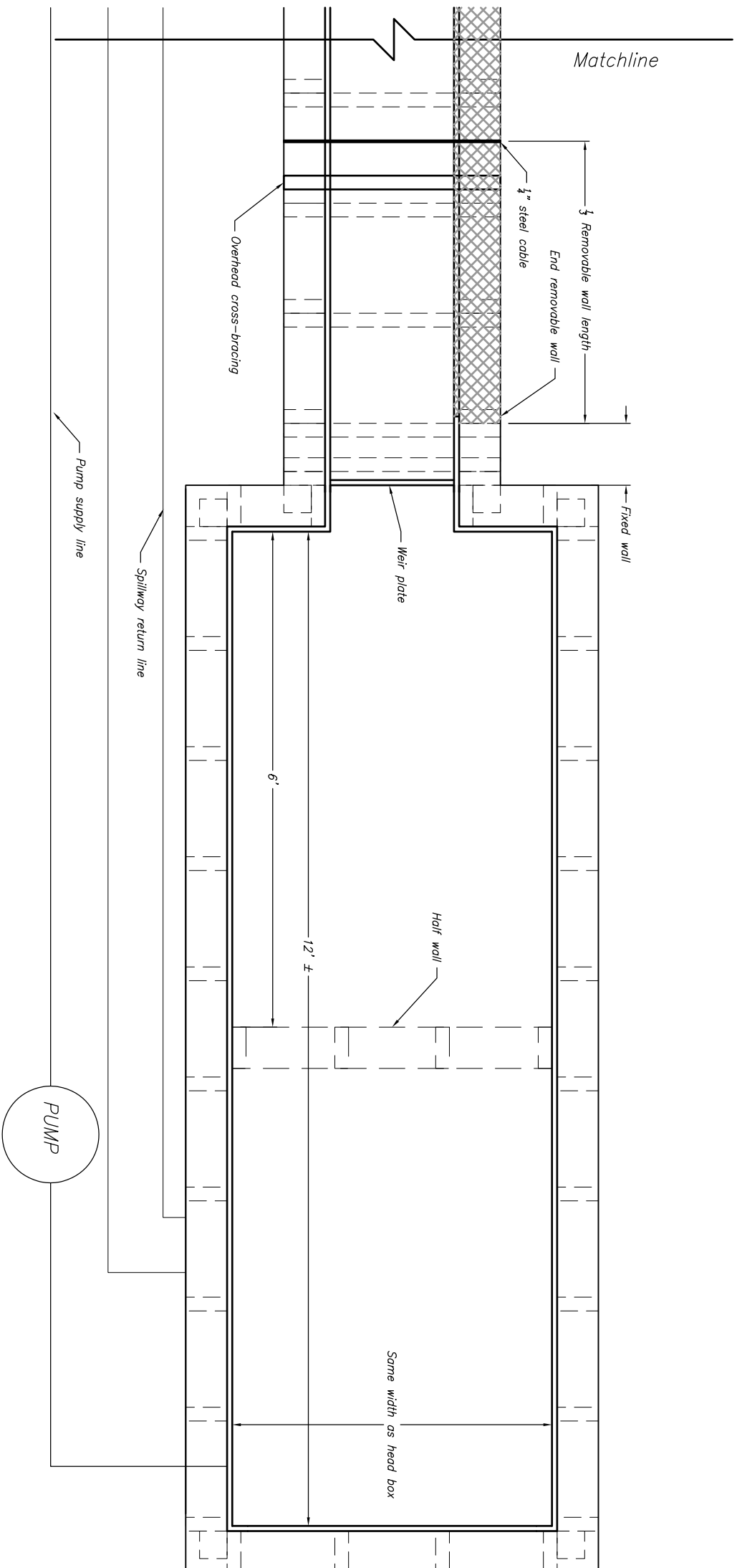
P. JERRY	DESIGNED
P. JERRY	DRAWN
OSWALD	CHECKED
T. HOWARD	TECH. SUPERV.
T. WAHL	ADMIN. APPROVAL

DENVER, CO 2014-12-03

CONTENTS (UP TO THREE LINES)

CEET-BOX-1

SHEET 2 OF 4



PLAN VIEW PART II



NOTES

1. Carpenters to determine head box and tail box interior dimensions based on minimum spillway widths.

P. IRBY	DESIGNED
P. IRBY	DRAWN
OSWALD	CHECKED
T. HOWARD	TECH. SUPERV.
T. WAHL	ADMIN. APPROVAL
DENVER, CO	2014-12-03

PLAN VIEW PART II

CEET-BOX-1

SHEET 3 OF 4



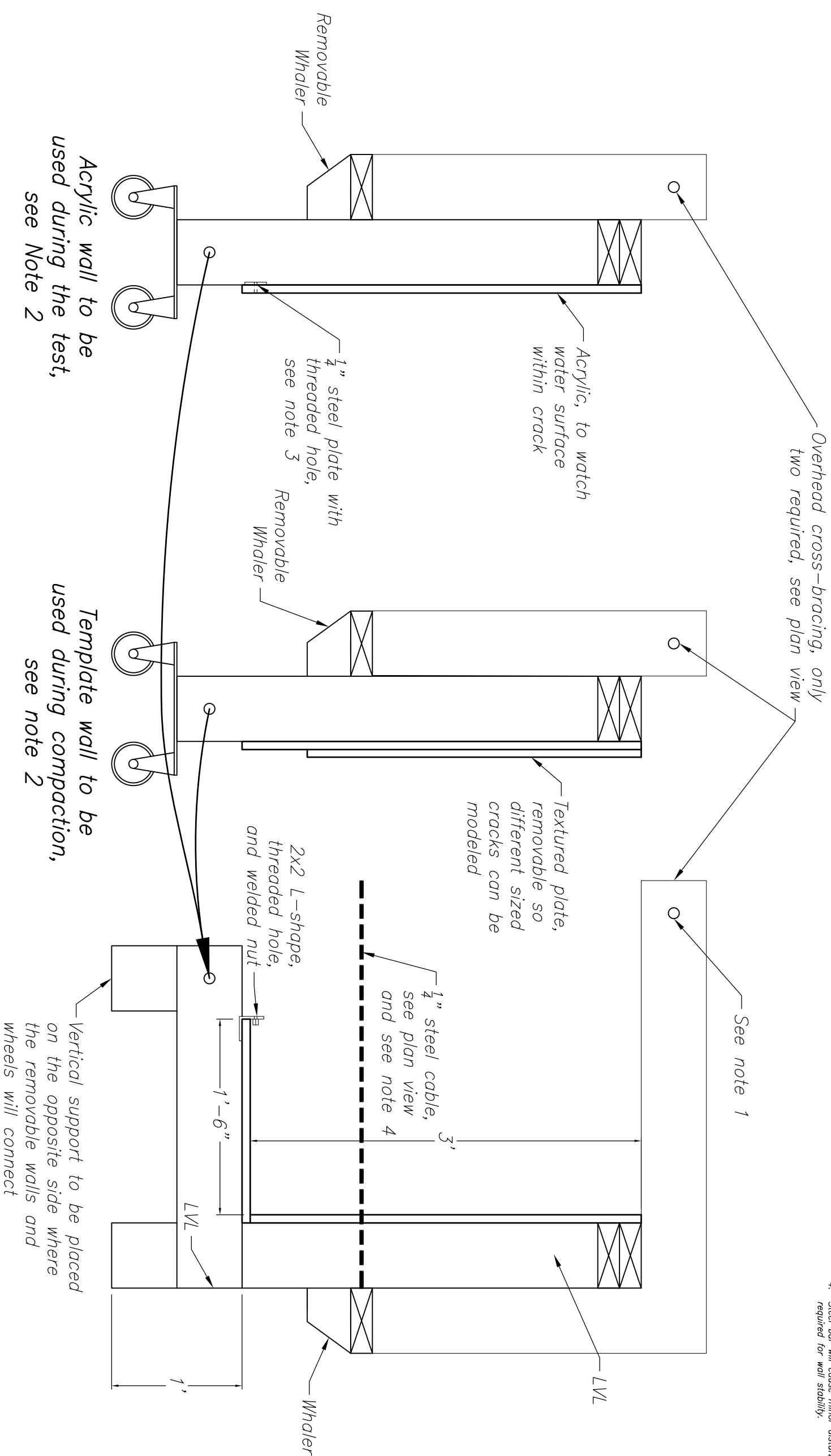
ALWAYS THINK SAFETY

U.S. DEPARTMENT OF THE INTERIOR
BUREAU OF RECLAMATION

EROSION RESEARCH
TECHNICAL SERVICES CENTER, COLORADO

CREST EMBANKMENT EROSION TEST
PROPOSED MODEL

- NOTES**
1. Carpenters to determine hole arrangement, multiple holes may be required.
 2. Two separate walls are to be constructed.
 3. When connecting the Acrylic Wall place 1" rubber stripping between plates and bolt to complete seal.
 4. Steel bar will cause minor disturbance and is required for wall stability.



SECTION VIEW

Acrylic wall to be used during the test, see Note 2

Template wall to be used during compaction, see note 2

Vertical support to be placed on the opposite side where the removable walls and wheels will connect

DESIGNED	P. IRBY
DRAWN	P. IRBY
CHECKED	T. HOWARD
TECH. DRAWN	T. HOWARD
ADMITTED APPROVAL	T. WAHL
DENVER, CO	2014-12-03

Appendix B

Material Properties



TEST REPORT

Prepared For:
USBR-Materials Engineering & Research Lab
P.O. Box 25007
Denver, CO 80225
303-445-2395

Report No.: 15121002
Material: Soil Samples
Project: Bonny Silt
Sampled By: Client
Attention: Mr. Robert Rinehart, P.E.

March 9, 2015
Page 1 of 10

ATTERBERG LIMITS & SPECIFIC GRAVITY (D4318 & D854: Method B)

<u>Sample</u>	<u>S. G.</u>	<u>LL</u>	<u>PL</u>	<u>PI</u>	<u>USCS*</u>
1	2.668	29	22	7	CL
2	2.675	26	21	5	CL-ML
3	2.675	26	22	4	ML
4	2.673	26	21	5	CL-ML
Composite of 1-4	2.675	27	21	6	CL-ML

*Classification based solely on Atterberg limit data.

STANDARD EFFORT COMPACTION (D698)

Data Attached.

PARTICLE-SIZE DISTRIBUTION (D422 & D6913)

Graphs & Tabulated Data Attached.

Rounding of values may cause slight differences in the sum of the percentages.



Report No.: 15121002
Material: Soil Samples
Project: Bonny Silt
Sampled By: Client
Attention: Mr. Robert Rinehart, P.E.

March 9, 2015
Page 2 of 10

Truck #1

U.S. Standard Sieve No.	Opening Size (mm)	Percent Passing
No. 4	4.75	100.0
No. 10	2.00	100.0
No. 20	0.840	99.9
No. 40	0.425	99.2
No. 60	0.250	97.7
No. 100	0.150	95.5
No. 140	0.106	93.2
No. 200	0.075	86.3
	Diameter	% Passing
	0.029	27.7
	0.021	19.3
	0.017	16.4
	0.013	13.3
	0.009	8.7
	0.007	7.7
	0.003	5.6
	0.001	4.0

Truck #2

U.S. Standard Sieve No.	Opening Size (mm)	Percent Passing
No. 4	4.75	100.0
No. 10	2.00	100.0
No. 20	0.840	99.9
No. 40	0.425	99.4
No. 60	0.250	97.9
No. 100	0.150	95.9
No. 140	0.106	94.0
No. 200	0.075	88.0
	Diameter	% Passing
	0.033	30.4
	0.022	16.9
	0.017	13.5
	0.013	8.9
	0.009	7.3
	0.007	4.4
	0.003	2.7
	0.001	2.0



Report No.: 15121002
Material: Soil Samples
Project: Bonny Silt
Sampled By: Client
Attention: Mr. Robert Rinehart, P.E.

March 9, 2015
Page 3 of 10

Truck #3

U.S. Standard Sieve No.	Opening Size (mm)	Percent Passing
No. 4	4.75	100.0
No. 10	2.00	100.0
No. 20	0.840	99.9
No. 40	0.425	99.7
No. 60	0.250	99.1
No. 100	0.150	97.8
No. 140	0.106	96.2
No. 200	0.075	90.6
	Diameter	% Passing
	0.033	31.1
	0.022	17.8
	0.017	13.1
	0.013	9.8
	0.009	7.1
	0.007	4.6
	0.003	2.5
	0.001	1.6

Truck #4

U.S. Standard Sieve No.	Opening Size (mm)	Percent Passing
No. 4	4.75	100.0
No. 10	2.00	100.0
No. 20	0.840	99.9
No. 40	0.425	99.5
No. 60	0.250	98.6
No. 100	0.150	97.1
No. 140	0.106	95.5
No. 200	0.075	90.4
	Diameter	% Passing
	0.032	30.8
	0.021	19.5
	0.017	15.0
	0.010	10.7
	0.009	9.1
	0.006	7.3
	0.003	5.9
	0.001	3.7



Report No.: 15121002
Material: Soil Samples
Project: Bonny Silt
Sampled By: Client
Attention: Mr. Robert Rinehart, P.E.

March 9, 2015
Page 4 of 10

Composite of 1-4

U.S. Standard Sieve No.	Opening Size (mm)	Percent Passing
No. 4	4.75	100.0
No. 10	2.00	100.0
No. 20	0.840	99.9
No. 40	0.425	99.5
No. 60	0.250	98.5
No. 100	0.150	96.9
No. 140	0.106	95.1
No. 200	0.075	89.2
	Diameter	% Passing
	0.033	41.1
	0.022	26.6
	0.018	21.3
	0.009	15.0
	0.007	12.8
	0.003	9.8
	0.001	6.6

6435 S. Routt St.
 Littleton, CO 80127
 Ph: 720-272-6282

Blue Rock Labs, Inc.

Project: Bonny Silt

Client: USBR

Sample Source: Composite of Samples 1-4

Supplier: _____

Test Information	
Project No.:	<u>15121002</u>
Test Date:	<u>03/04/15</u>
Proctor No.:	_____
Test Method:	<u>ASTM D 698 Method A</u>
Rammer Type:	<u>Manual</u>
Prep. Method:	<u>Moist</u>

Sample Description
<u>Light brown, silt to silty clay with organics</u>

Sample Properties	
Moisture Content	<u>9.6</u>
Liquid Limit	<u>27</u>
Plastic Limit	<u>21</u>
Plasticity Index	<u>6</u>
Specific Gravity:	<u>2.675</u> Actual
Classification	<u>CL-ML</u>

Test Results:	
Maximum Dry Unit Weight (pcf):	<u>105.2</u>
Optimum Water Content (%):	<u>17.0</u>
Oversize Correction Values:	
Maximum Dry Unit Weight (pcf):	<u>--</u>
Optimum Water Content (%):	<u>--</u>

Tested By: KA

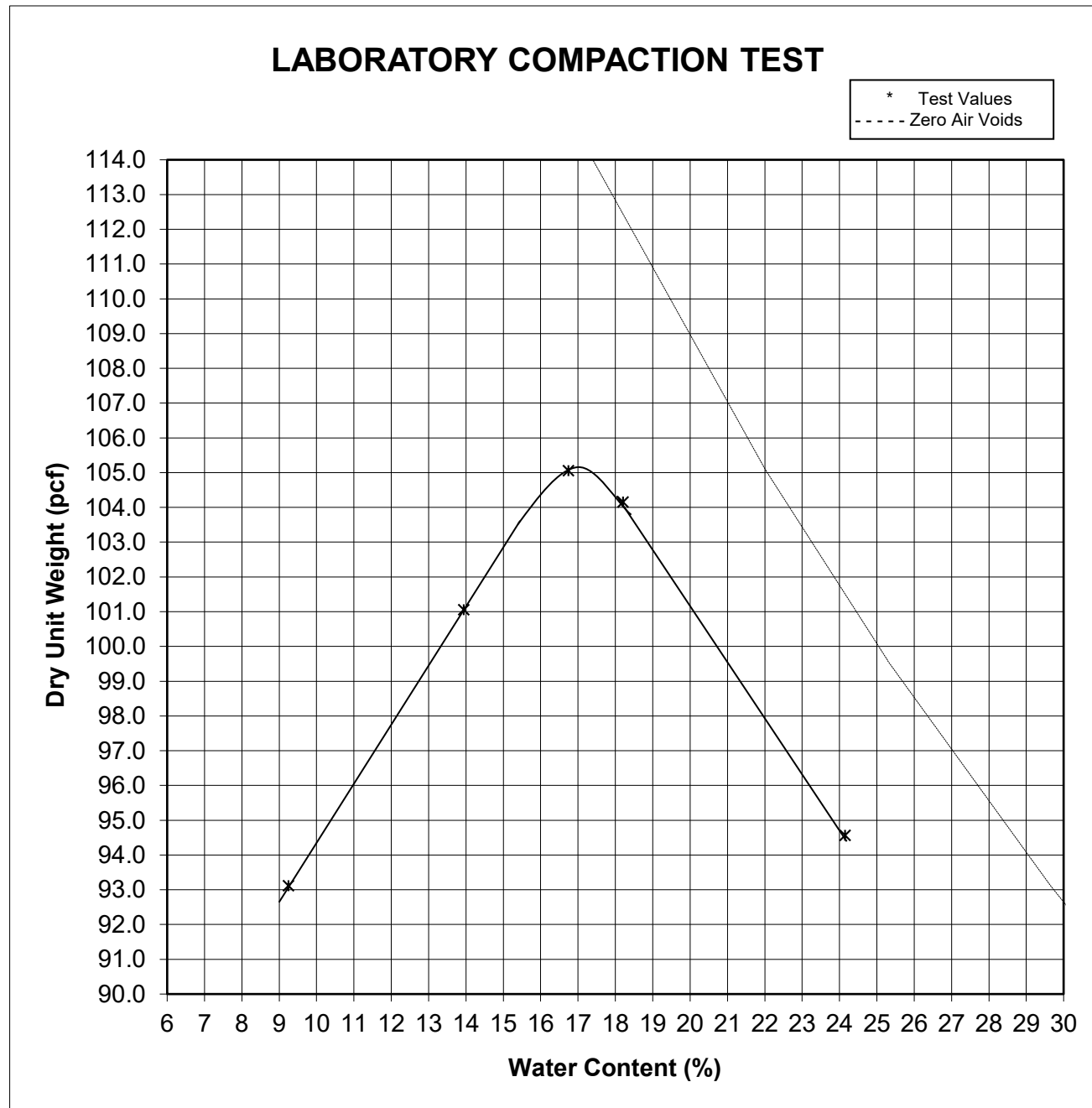
Input By: KA

Date: 03/04/15

Date: 03/06/15

Checked By: KA

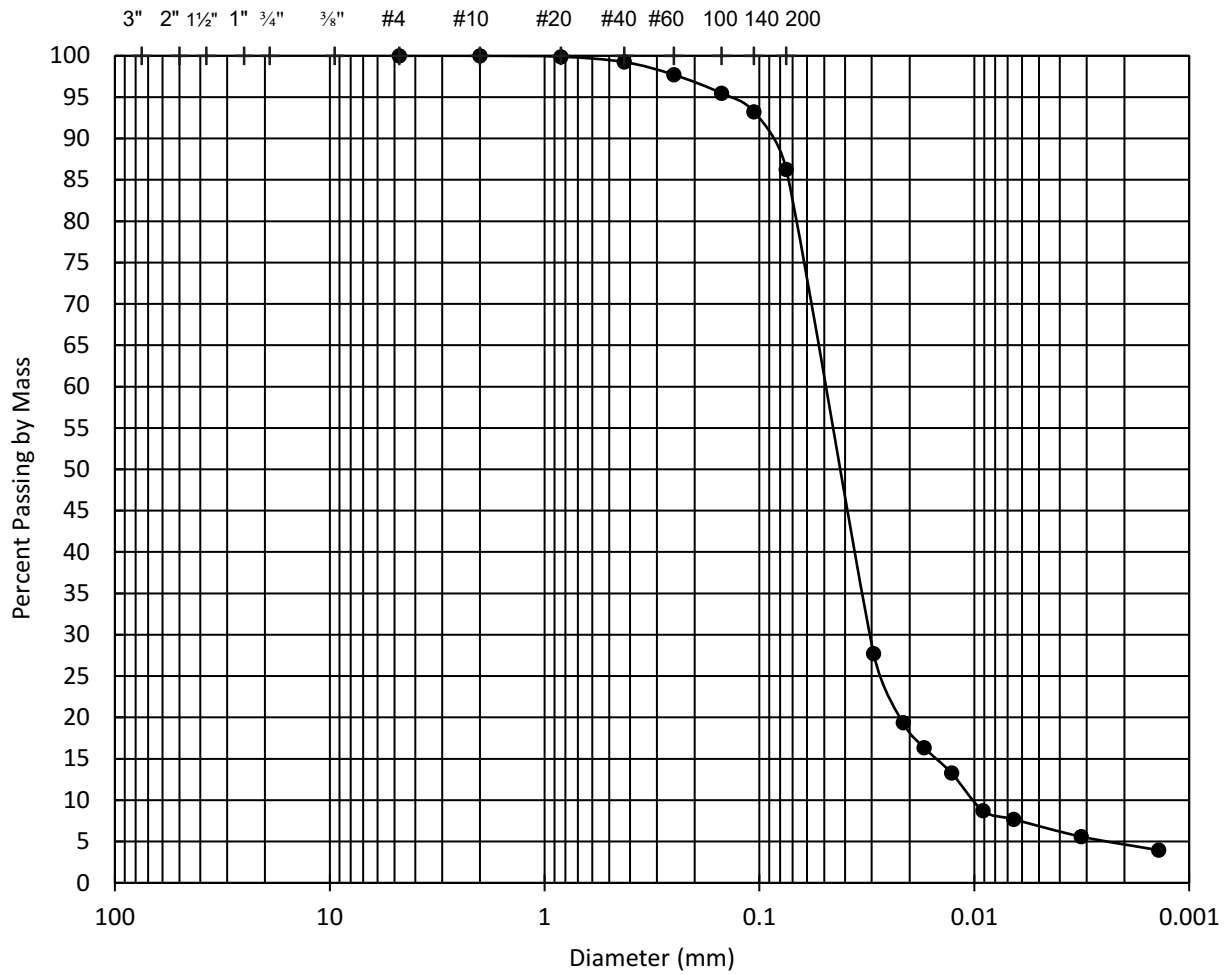
Date: 03/07/15





Blue Rock Labs, Inc.

**PARTICLE SIZE DISTRIBUTION
ASTM D6913**



Cobbles	Gravel		Sand			Fines	
	Coarse	Fine	Coarse	Medium	Fine	Silt	Clay

Cobbles (%)	Gravel (%)		Sand (%)			Fines (%)	
			13.7			86.3	
	Coarse	Fine	Coarse	Medium	Fine	Silt	Clay
				0.8	13.0	79.5	6.7

Project No.: 15121002

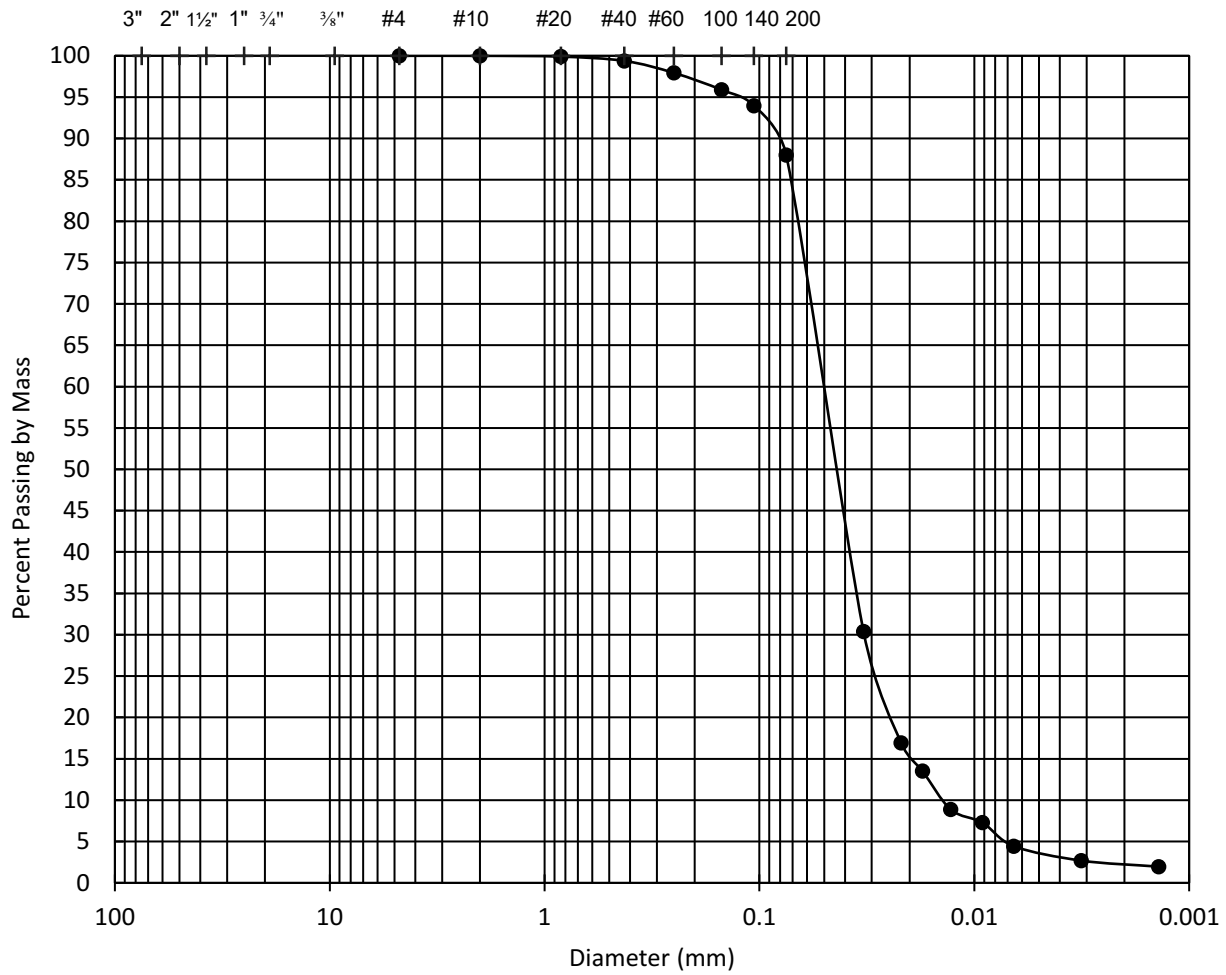
Boring: Bonny Silt

Sample: 1



Blue Rock Labs, Inc.

PARTICLE SIZE DISTRIBUTION ASTM D6913



Cobbles	Gravel		Sand			Fines	
	Coarse	Fine	Coarse	Medium	Fine	Silt	Clay

Cobbles (%)	Gravel (%)		Sand (%)			Fines (%)	
			12.0			88.0	
	Coarse	Fine	Coarse	Medium	Fine	Silt	Clay
				0.6	11.4	84.3	3.6

Project No.: 15121002

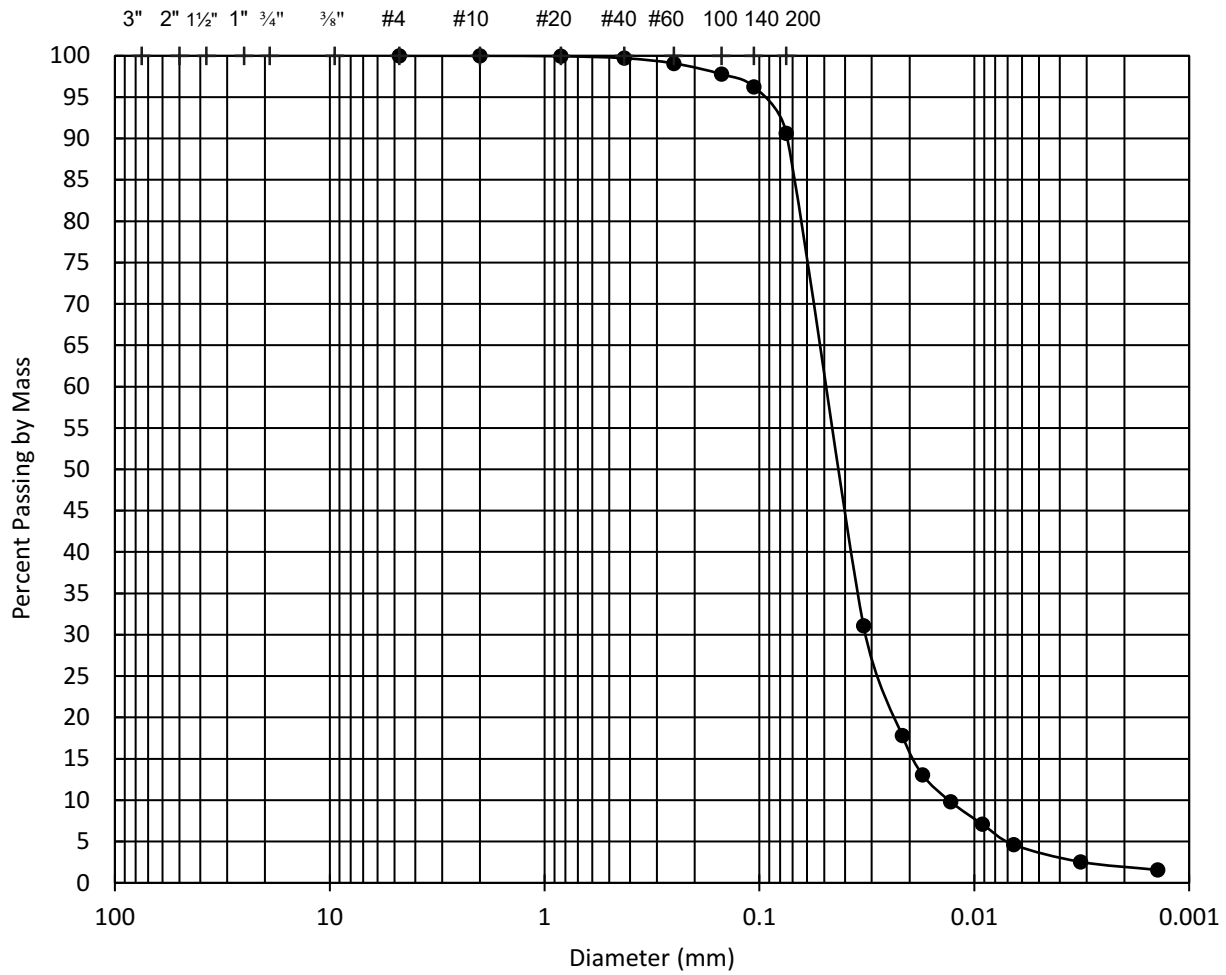
Boring: Bonny Silt

Sample: 2



Blue Rock Labs, Inc.

PARTICLE SIZE DISTRIBUTION ASTM D6913



Cobbles	Gravel		Sand			Fines	
	Coarse	Fine	Coarse	Medium	Fine	Silt	Clay

Cobbles (%)	Gravel (%)		Sand (%)			Fines (%)	
			9.4			90.6	
	Coarse	Fine	Coarse	Medium	Fine	Silt	Clay
				0.3	9.1	87.0	3.6

Project No.: 15121002

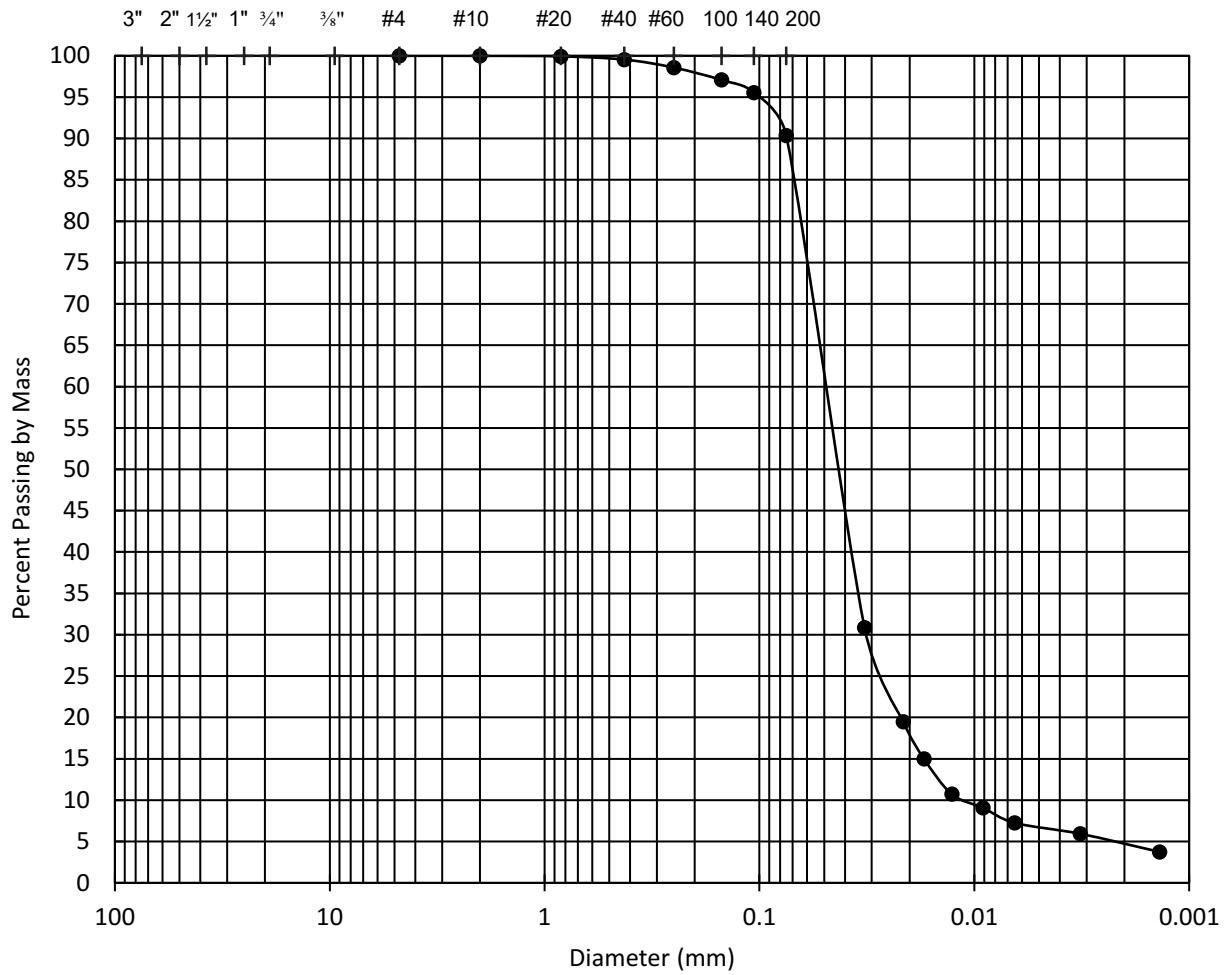
Boring: Bonny Silt

Sample: 3



Blue Rock Labs, Inc.

**PARTICLE SIZE DISTRIBUTION
ASTM D6913**



Cobbles	Gravel		Sand			Fines	
	Coarse	Fine	Coarse	Medium	Fine	Silt	Clay

Cobbles (%)	Gravel (%)		Sand (%)			Fines (%)	
			9.6			90.4	
	Coarse	Fine	Coarse	Medium	Fine	Silt	Clay
				0.5	9.2	83.7	6.7

Project No.: 15121002

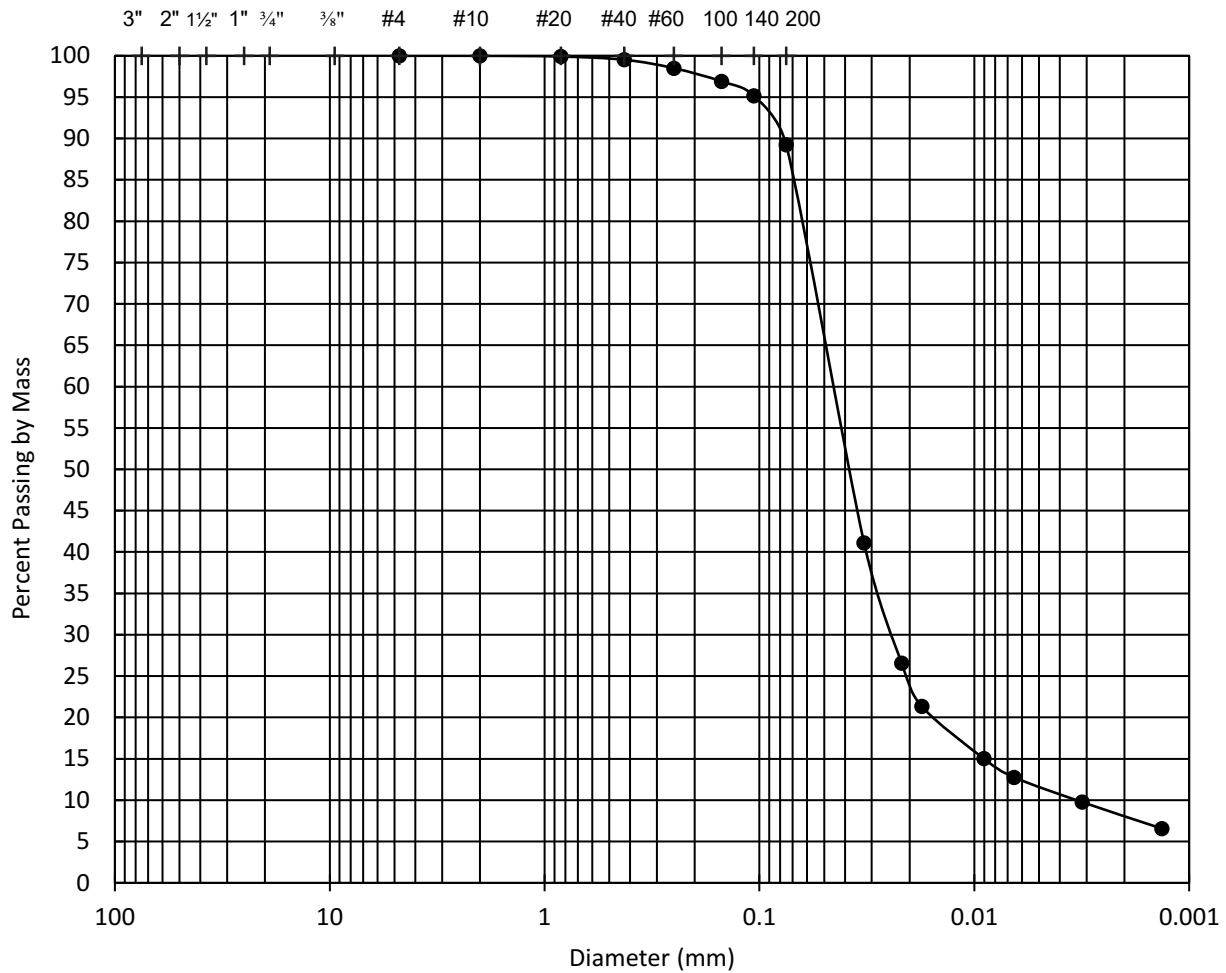
Boring: Bonny Silt

Sample: 4



Blue Rock Labs, Inc.

**PARTICLE SIZE DISTRIBUTION
ASTM D422 & D6913**

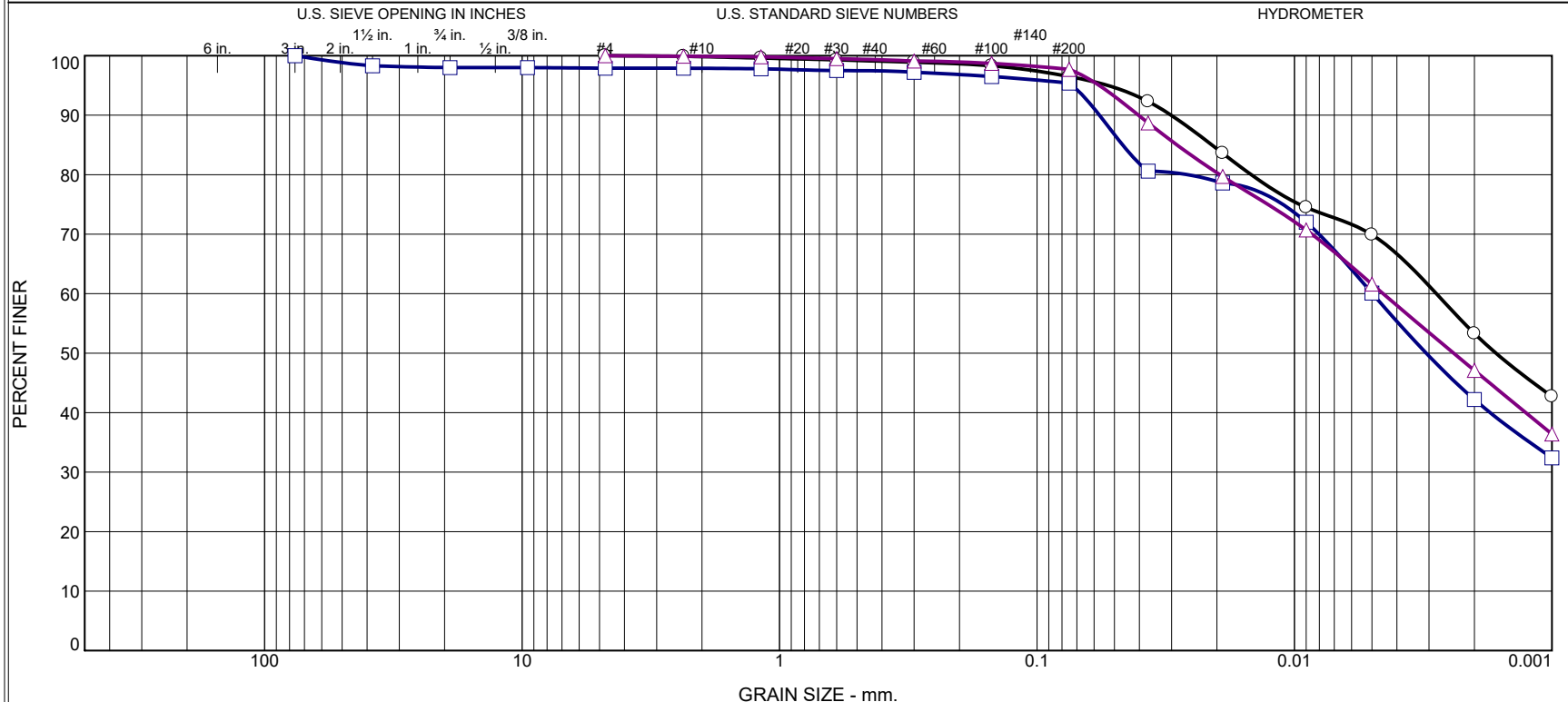


Cobbles	Gravel		Sand			Fines	
	Coarse	Fine	Coarse	Medium	Fine	Silt	Clay

Cobbles (%)	Gravel (%)		Sand (%)			Fines (%)	
			10.8			89.2	
	Coarse	Fine	Coarse	Medium	Fine	Silt	Clay
				0.5	10.3	77.8	11.4

Project No.: 15121002
 Project Name: Bonny Silt
 Sample: Composite 1-4

Particle Size Distribution Report



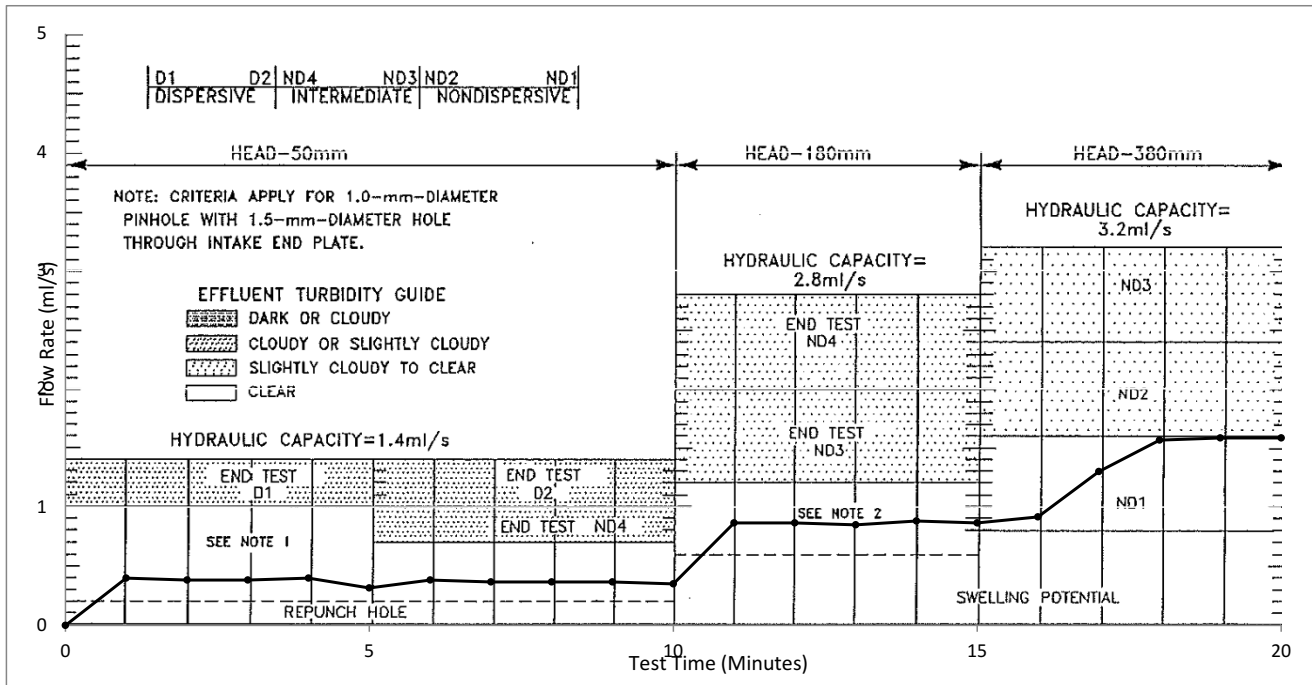
	% Cobbles	% Gravel		% Sand			% Fines	
		Coarse	Fine	Coarse	Medium	Fine	Silt	Clay
○	0.0	0.0	0.0	0.2	0.7	2.6	43.2	53.3
□	0.0	2.0	0.1	0.0	0.4	2.1	53.2	42.2
△	0.0	0.0	0.0	0.1	0.6	1.6	50.6	47.1

Source	Sample #	Depth/Elev.	Date Sampled	USCS	Material Description	NM %	LL	PL
Highland Clay	Clod		12-2-2016	CH	CH - Fat Clay, "Clod" Sample		53	25
Highland Clay	Composite			CH	CH/CL - Borderline Fat to Lean Clay, Composite of both trucks.		50	23
Highland Clay	Loose		12-2-2016	CL	CL - Lean Clay, "Loose" sample		48	26

Client S&T	BUREAU OF RECLAMATION	○ SpG -#4 = 2.73 □ SpG of -#4 = 2.72 △ SpG -#4 = 2.72
Project Cracked Embankment Erosion Testing		
Project No. CEET Figure		
Denver, Colorado		

Tested By: ○ Armstrong □ Hironaka △ Armstrong Checked By: Chatfield

PINHOLE TEST - DISPERSIVE VERSUS FLOW RATE



Note 1: Flow rate < 1.0 ml/s continue test at 50mm head for 5 more minutes.

Note 2: Flow rate of 0.6 to 1.2 ml/s increase head and continue test.

DISPERSIVE GRADE VS FLOW RATE

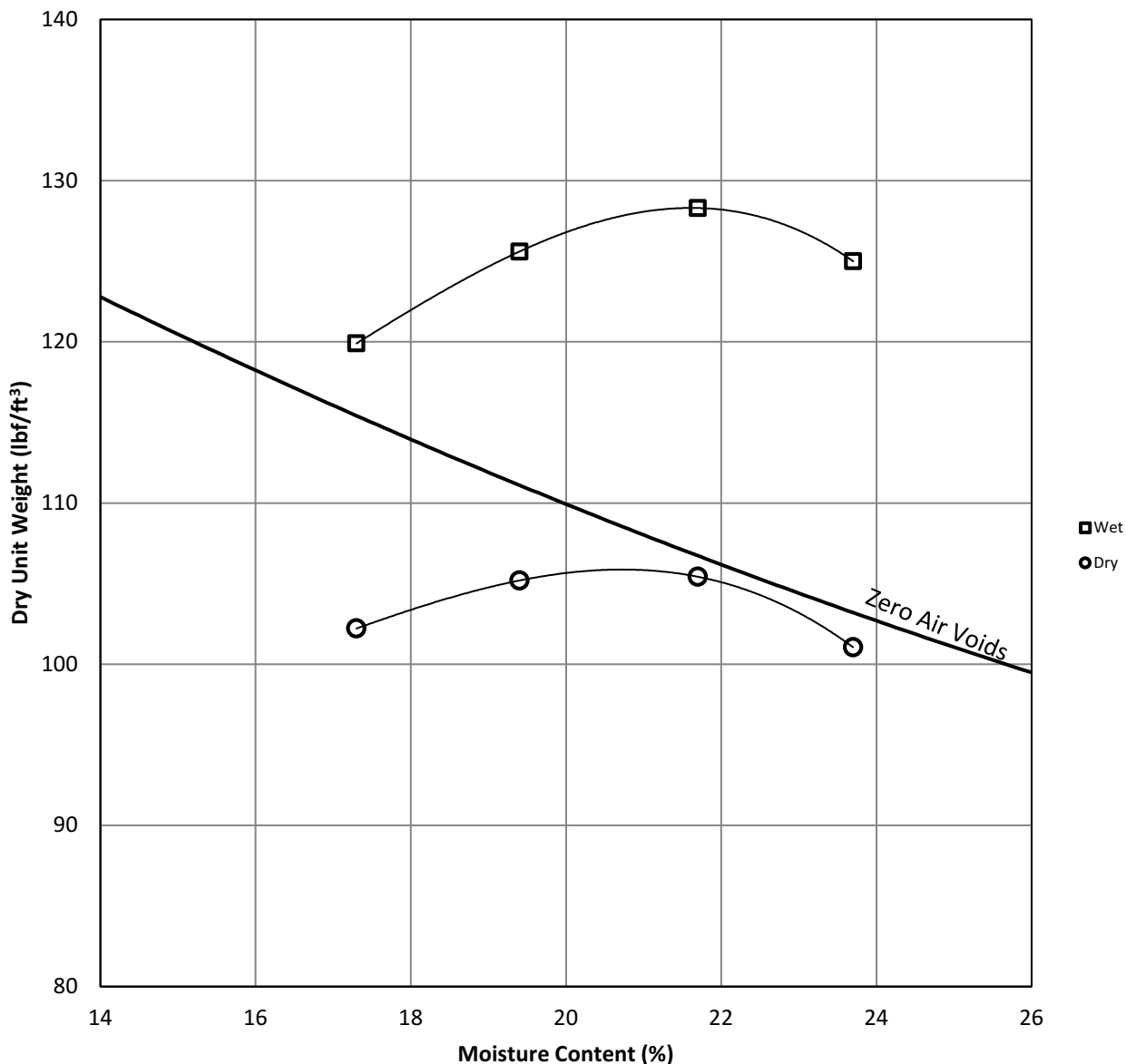
Sample Number	Placement Conditions		Dispersive Grade Classification
	Dry Density	Water Content	
Crack Box Specimen	105.3 pcf	21.22%	ND2

Laboratory Compaction Test - Standard Effort

Blows per Layer 25
 No. of Layers 3
 Height of drop (in) 12

Mass of tamping rod (lb) 5.5
 Volume of Mold (ft³) 0.0332

Date 15-Nov-16



Project CEET
Feature NA
Location Bldg 56 Stockpile
Depth (ft) NA
Sample No. Clay

Specific Gravity
Minus No. 4 2.72
Plus No. 4
Bulk
Apparent
Absorption (%)

Compaction
Percent larger than tested 2.1
Maximum Dry Unit Weight (lb/ft³) 106.0
Optimum Moisture Content (%) 20.7
Degree of saturation @ opt (%) 93.8

Classification CH/CL
Gravel (%) 2.1
Sand (%) 2.5
Fines(%) 95.4

Atterberg Limits
Liquid Limit 50
Plasticity Index 27
Shrinkage Limit

Remarks: As-received water content of 21.6%

Tested By: Hironaka

Checked By: Rinehart

Appendix C

Summary of Tests 3 through 9

Summary of Large Scale Testing Results

Material Type	Test Number	Dry Unit Weight	Average Dry Unit Weight	Percent Compaction	Average Percent Compaction	Moisture Content	Average Moisture Content	Void Ratio	Average Void Ratio	Degree of Saturation (at time of compaction)	Average Degree of Saturation	Comments
Bonny Silt	1A	97.63	99.68	92.8%	94.7%	13.59	16.53	0.71	0.68	51.22	65.98	~ 9-inches high
	1B	105.42		100.2%		17.00		0.58		77.95		~ 12.5-inches high
	1C	95.98		91.2%		19.00		0.74		68.76		~ 31-inches high
Bonny Silt	2A	89.219	96.56	84.8%	91.8%	18.30	18.14	0.87	0.74	56.21	67.75	~ 12.5-inches high, only went 1-2inches below surface
	2B	103.9		98.8%		17.98		0.61		79.30		~25-inches high
Bonny Silt	3A	96.88	99.49	92.1%	94.6%	18.70	18.69	0.72	0.68	69.19	73.85	Center ~ 20-inches from top
	3B	101.1		96.1%		17.78		0.65		73.05		
	3C	100.49		95.5%		19.60		0.66		79.31		3rd step DS
Bonny Silt	4A	98.54	97.47	93.7%	92.7%	18.40	19.05	0.69	0.71	70.93	71.48	removing 2nd DS step
	4B	96.4		91.6%		19.70		0.73		72.04		removing 3rd DS step
Bonny Silt	5A	107.7	106.65	102.4%	101.4%	16.80	17.02	0.55	0.57	81.73	80.55	2nd DS step
	5B	105.6		100.4%		17.23		0.58		79.37		
Bonny Silt	6A	107.6	110.31	102.3%	104.9%	14.15	13.45	0.55	0.51	68.63	70.00	1st DS step
	6B	113.0		107.4%		12.15		0.48		68.17		2nd DS step
	6C	Just a moisture sample				14.04		0.51		73.20		Moisture sample
Highland Clay	7A	107.91	108.23	101.8%	102.1%	16.80	17.05	0.57	0.57	79.77	81.62	1st DS step
	7B	108.54		102.4%		17.30		0.56		83.47		2nd DS step
Highland Clay	8A	99.825	101.59	94.2%	95.8%	20.20	20.18	0.70	0.67	78.46	81.90	removing 2nd DS step
	8B	103.35		97.5%		20.15		0.64		85.34		removing 3rd DS step
Highland Clay	9A	94.8	96.25	89.4%	90.8%	24.00	23.45	0.79	0.76	82.59	83.54	1st DS step
	9B	97.7		92.2%		22.90		0.74		84.49		2nd DS step

Test 1 through 3

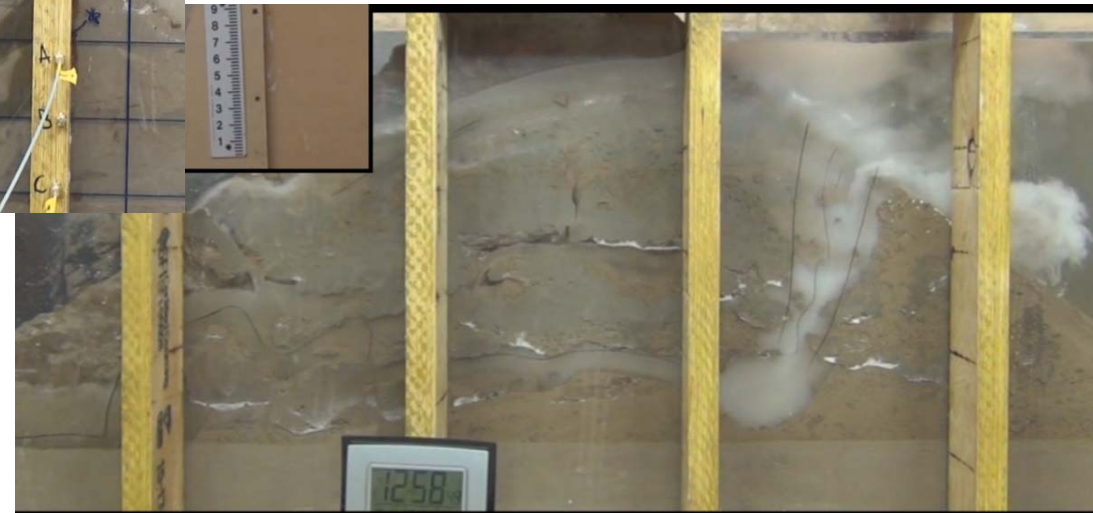
- **Bonny Silt**
 - Test 3 added steel, pressure gauges, had a varying reservoir

Test 1 Bonny Silt 95%comp, 16.5%MC



Test 3 Bonny Silt 95%comp, 18.7%MC

- Tests 1 through 3 are considered trials and were not used in the results



Test 2 Bonny Silt 92%comp, 18%MC

Test 4 through 6

Test 5 Bonny Silt 101%comp, 17.0%MC



Test 4 Bonny Silt 93%comp, 19.0%MC

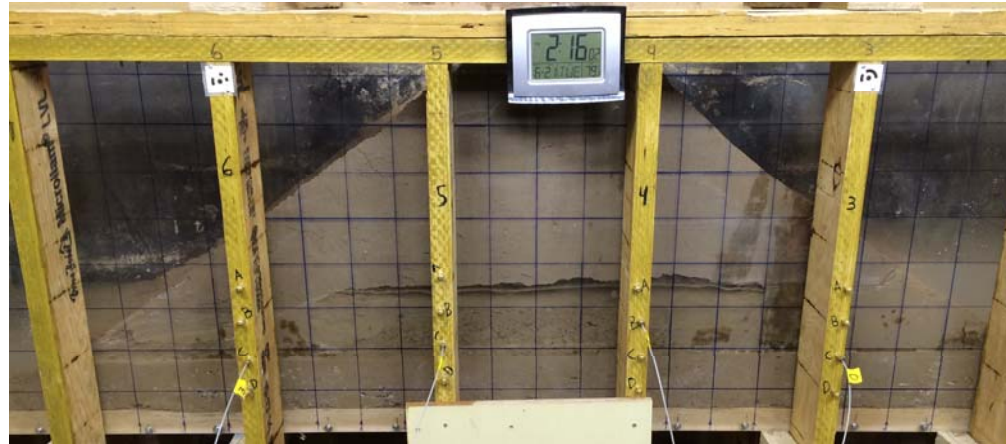


Test 6 Bonny Silt 104%comp, 13.0%MC



- Global Gradient ~ 0.08

Test 4



• Observations during Test 4

- Erosion started approximately 50 minutes after water entered the crack, behind post 4.
- Lowly spread upstream and downstream.
- Clods deposited in crack.
- Lowering of water for photogrammetry disturbed clods.
- After 12 hours the clods were slowly removed from the system.
 - Roof began collapsing after 12 to 16 hours, very large clods collapsed and were carried downstream.
- Reservoir remained constant at 8 inches above the bottom of the crack. Except when lowered for photogrammetry

- Compacted to 93%, placed at 2% wet of optimum
- Global Gradient ~ 0.08 , $P(\text{Erosion}) = 0.3$ to 1.0
- Erosion Started after 50 minutes
 - 172 in³ eroded after 3 hours
 - 186 in³ eroded after 6.25 hours
 - 856 in³ eroded after 21.25 hours
 - 2354 in³ eroded after 28 hours
 - Average erosion rate = 53 in³/hour

Test 5



- **Compacted to 101%, placed at optimum**
- **Global Gradient ~ 0.08 , $P(\text{Erosion}) = 0.3$ to 1.0**
- **Erosion Started after 5 minutes**
 - 116 in^3 eroded after 0.83 hours
 - 820 in^3 eroded after 3.0 hours
 - 1448 in^3 eroded after 4.5 hours
 - Average erosion rate = $245 \text{ in}^3/\text{hour}$

• Observations during Test 5

- Erosion started immediately where the water entered the crack.
- After 45 minutes erosion began between posts 6, 5, and 4 moving upstream towards the reservoir.
- Clods were smaller than Test 4 and did NOT deposit in crack.
- Erosion path was downward not just horizontal.
- No large collapse like when roof collapsed in Test 4.
- Reservoir remained constant at 8 inches above the bottom of the crack. Except when lowered for photogrammetry

Test 6



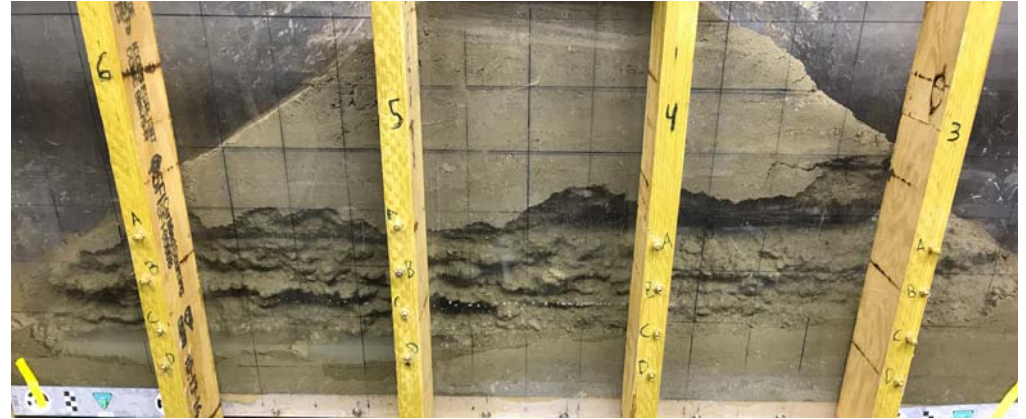
• Observations during Test 6

- Erosion started immediately where the water entered the crack.
- Erosion began at the base of the crack between posts 5 and 4.
- Clods were very small, material appeared explosive.
- Pipe formed from upstream to downstream in less than 20 minutes (note 485 in³ in 0.3 hours!)
- Erosion was downwards and into the embankment. Extended more than 12 inches into the embankment

- Compacted to 105%, placed at 3.5% dry of optimum
- Global Gradient ~ 0.08 , $P(\text{Erosion}) = 0.3$ to 1.0
- Erosion Started after 2 minutes
 - 485 in³ eroded after 0.3 hours
 - 1740 in³ eroded after 2.0 hours
 - Test ran for an additional 1 hr, embankment collapsed when wall removed for final volume.
 - Average erosion rate = 1,163 in³/hour

Test 7 through 9

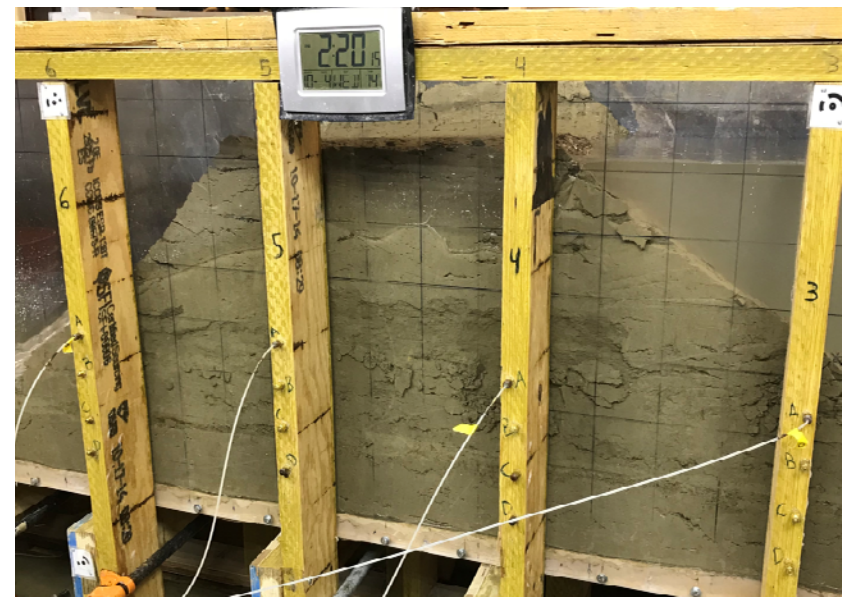
Test 7 Highland Clay 102%comp, 17.0%MC



Test 8 Highland Clay 96%comp, 20.0%MC

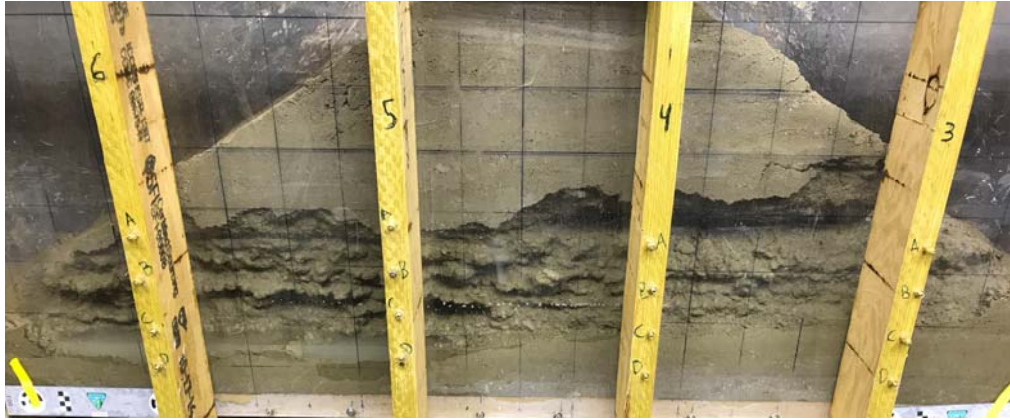


Test 9 Highland Clay 91%comp, 23.5%MC



- **Global Gradient ~ 0.08**
- **Foster and Fell Tables**
 - $P(\text{Erosion}) = 0.03 \text{ to } 0.4$

Test 7



• Observations during Test 7

- Erosion started immediately where the water entered the crack.
- Erosion began anywhere water encountered the material. Erosion was continuous from US to DS didn't just occur at one location
- Clods were very small, material appeared explosive.
- Clods deposited in crack even though they were small.
- A few large Clods between posts 5 and 6 caused average gradient to flatten.
 - Large clods were eventually washed out. Along with smaller clods deposited in channel.

- Compacted to 102%, placed at 3.7% dry of optimum
- Global Gradient ~ 0.08 , $P(\text{Erosion}) = 0.03$ to 0.4
- Erosion started after immediately (explosive)
 - 696 in^3 eroded after 2.25 hours
 - 2282 in^3 eroded after 3.0 hours
 - Average erosion rate = $535 \text{ in}^3/\text{hour}$

Test 8

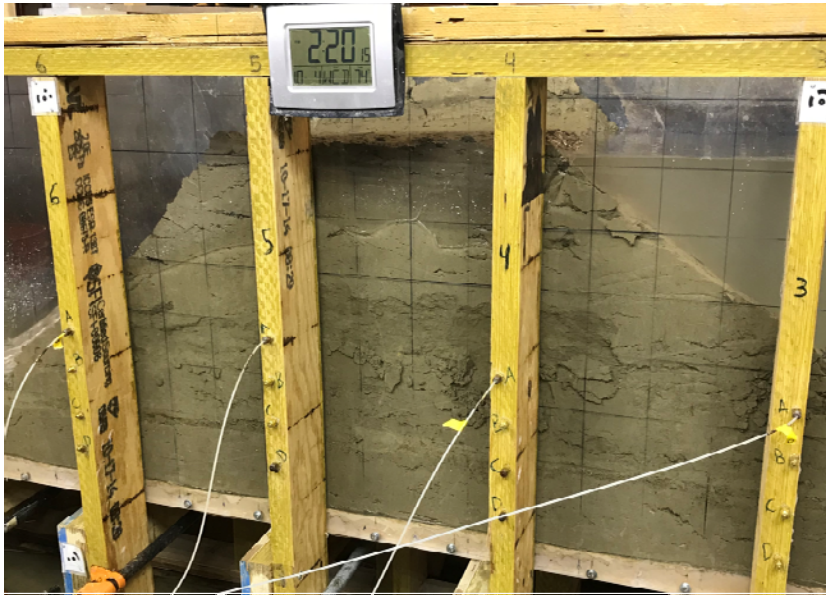


• Observations during Test 8

- Erosion started quickly.
- Erosion began between posts 6 and 3. Erosion was continuous from US to DS didn't just occur at one location
- Clods were small and large.
- Clods deposited in crack.
- Enough clods deposit in the crack that the gradient became flat and after ~40 hours almost no flow past through the crack.
 - Considered the crack to be self-healed at this point and the reservoir was increased flushing out clods from the crack.
- Reservoir was increased to the full height after 48hrs for 45 minutes. Note that the last eroded volume measurement is largely influenced by the high erosion rates that occurred at the higher reservoir.

- **Compacted to 96%, placed at 0.5% dry of optimum**
- **Global Gradient ~0.08, P(Erosion) = 0.03 to 0.4, Reservoir Increased after Self healing**
- **Erosion Started after 2 minutes**
 - 12 in³ eroded after 1.5 hours
 - 921 in³ eroded after 43 hours
 - Average erosion rate = 17 in³/hour
 - **NOTE**
 - Flow less than 1 gpm after 20 hours. Lost reservoir 35 hours into test
 - Reservoir raised after 38 hrs of water flowing through crack. Gradient increased to 0.2

Test 9



• Observations during Test 8

- Erosion occurred very slowly and after 5 hours with water in the crack.
- Erosion began between posts 4 and 3. Very little erosion occurred.
- Clods were large
- Virtually no erosion occurred in the first 15 hours.
- Majority of the 85 in³ measure occurred at the higher reservoir.
- Erosion rates significantly impacted by the increased reservoir. At a gradient of 0.1 erosion rate might have only been 1 in³/hour
- Erosion occurred in large clods that quickly became stuck in the crack.

- **Compacted to 91%, placed at 2.8% wet of optimum**
- **Global Gradient ~0.08, P(Erosion) = 0.03 to 0.4, Reservoir Increased after no erosion for 24hrs**
- **Erosion Started after 20 hours**
 - 85 in³ eroded after 19 hours (0.1 gradient for 15 hours, 0.25 for 4 hours)
 - 268 in³ eroded after 59 hours (0.1 gradient for 15 hours, 0.25 for 24 hours, 0.3 for 20 hours)
 - Average erosion rate = 5 in³/hour
 - **NOTE**
 - Lost gradient between 9 hours to 18 hours

Appendix D
Video Summary of Each Large-Scale Test
(Digital Files)

Appendix E

JET and HET results

Bonny Silt JETs

Water Content (%)	Dry Unit Weight (pcf)	Saturation (%)	Void Ratio	Compaction Method	k_d (ft/hr/psf)	τ_c (psf)
13%	103.5	54%	0.6	Standard Proctor	78.5	0.00068
13%	101.6	54%	0.6	Standard Proctor	74.3	0.00005
13%	103.3	56%	0.6	Standard Proctor	71.2	0.00008
15%	106.2	74%	0.6	Standard Proctor	8.2	0.034
15%	106.3	72%	0.6	Standard Proctor	9.1	0.026
15%	106.0	75%	0.6	Standard Proctor	7.2	0.040
15%	NA	NA	NA	Standard Proctor	5.6	0.00137
15%	NA	NA	NA	Standard Proctor	6.6	0.00083
15%	NA	NA	NA	Standard Proctor	5.3	0.00113
15%	110.7	78%	0.5	Modified Proctor	4.5	0.00045
15%	110.5	78%	0.5	Modified Proctor	4.6	0.00021
15%	111.4	80%	0.5	Modified Proctor	3.5	0.00022
15%	110.3	77%	0.5	Modified Proctor	4.6	0.00023
15%	110.1	77%	0.5	Modified Proctor	4.8	0.00043
15%	110.8	78%	0.5	Modified Proctor	4.5	0.00022
15%	104.6	67%	0.6	Modified Proctor	4.0	0.00143
15%	110.8	78%	0.5	Modified Proctor	7.9	0.00006
15%	111.5	80%	0.5	Modified Proctor	4.0	0.00026
17%	108.8	77%	0.5	Standard Proctor	6.4	0.026
17%	108.6	79%	0.5	Standard Proctor	12.8	0.026
17%	108.6	81%	0.5	Standard Proctor	7.7	0.036
17%	105.0	76%	0.6	Standard Proctor	10.2	0.00004
17%	104.3	75%	0.6	Standard Proctor	8.8	0.00006
17%	104.7	75%	0.6	Standard Proctor	10.2	0.00003
17%	NA	NA	NA	Standard Proctor	3.7	0.0035
17%	NA	NA	NA	Standard Proctor	4.0	0.0021
17%	NA	NA	NA	Standard Proctor	4.2	0.0018
17%	110.9	89%	0.5	Modified Proctor	1.3	0.0033
17%	112.8	94%	0.5	Modified Proctor	1.4	0.0019
17%	111.9	91%	0.5	Modified Proctor	0.9	0.0044
19%	105.9	87%	0.6	Standard Proctor	0.8	0.003
19%	106.3	88%	0.6	Standard Proctor	0.9	0.007
19%	105.8	87%	0.6	Standard Proctor	0.4	#####
19%	100.2	83%	0.6	Standard Proctor	9.6	0.040
19%	102.0	84%	0.6	Standard Proctor	24.2	0.030
19%	101.6	84%	0.6	Standard Proctor	11.3	0.0040
19%	NA	NA	NA	Standard Proctor	10.8	0.00009
19%	NA	NA	NA	Standard Proctor	11.4	0.00009
19%	NA	NA	NA	Standard Proctor	6.0	0.00029
19%	101.3	77%	0.6	Standard Proctor	10.2	0.00004
19%	101.3	77%	0.6	Standard Proctor	9.2	0.00010
19%	107.9	92%	0.5	Modified Proctor	3.1	0.0007
19%	107.8	92%	0.5	Modified Proctor	3.4	0.00041
19%	107.9	92%	0.5	Modified Proctor	3.4	0.00038
21%	102.4	94%	0.6	Standard Proctor	0.9	0.006
21%	101.8	95%	0.6	Standard Proctor	0.6	0.018
21%	102.4	94%	0.6	Standard Proctor	0.3	0.099

NA = not available (records of unit weight were lost)

Highland Clay JETs							
Water Content (%)	Dry Unit Weight (pcf)	Saturation (%)	Void Ratio	Compaction Method	k_d (ft/hr/psf)	τ_c (psf)	Initial Pressure Head
17%	97.7	62%	0.7	Standard Proctor	0.83	0.0028	High Head
17%	98.8	63%	0.7	Standard Proctor	0.44	0.0047	High Head
17%	96.8	60%	0.8	Standard Proctor	0.52	0.22	High Head
17%	103.0	71%	0.6	Standard Proctor	1.3	0.0008	Low Head
17%	105.4	76%	0.6	Standard Proctor	0.8	0.0006	Low Head
17%	104.9	75%	0.6	Standard Proctor	1.3	0.0004	Low Head
19%	106.1	85%	0.6	Standard Proctor	0.17	0.0195	Low Head
19%	106.4	85%	0.6	Standard Proctor	0.29	0.0087	Low Head
19%	106.4	87%	0.6	Standard Proctor	0.21	0.0104	Low Head
19%	101.2	73%	0.7	Standard Proctor	0.064	0.20	High Head
19%	101.8	74%	0.7	Standard Proctor	0.10	0.11	High Head
19%	98.5	70%	0.7	Standard Proctor	0.21	0.18	High Head
21%	105.5	92%	0.6	Standard Proctor	0.14	0.015	Low Head
21%	105.4	92%	0.6	Standard Proctor	0.16	0.020	Low Head
21%	105.3	92%	0.6	Standard Proctor	0.19	0.013	Low Head
21%	104.3	89%	0.6	Standard Proctor	0.0053	1.8	High Head
21%	103.9	89%	0.6	Standard Proctor	0.0092	1.0	High Head
21%	103.1	86%	0.6	Standard Proctor	0.015	0.23	High Head
23%	100.5	90%	0.7	Standard Proctor	0.22	0.0083	Low Head
23%	102.3	94%	0.7	Standard Proctor	0.21	0.013	Low Head
23%	102.3	94%	0.7	Standard Proctor	0.30	0.0022	Low Head
23%	102.8	94%	0.7	Standard Proctor	0.0016	8.1	High Head
23%	102.4	92%	0.7	Standard Proctor	0.0039	3.3	High Head
23%	102.9	95%	0.6	Standard Proctor	0.0028	3.9	High Head
25%	102.6	96%	0.7	Standard Proctor	0.0025	3.1	High Head
25%	102.2	95%	0.7	Standard Proctor	0.0021	1.4	High Head
25%	102.4	96%	0.7	Standard Proctor	0.0025	1.6	High Head

Bonny Silt HETs

Water Content (%)	Dry Unit Weight (pcf)	Satruation (%)	Void Ratio	Compaction Method	k_d (ft/hr/psf)	τ_c (psf)	I_{HET}
15%	102.8	63%	0.63	Standard Proctor	2.5	6.0	2.1
15%	108.8	74%	0.54	Standard Proctor	0.12	1.5	3.4
15%	No Erosion Intiated						
17%	No Erosion Intiated						
17%	104.3	75%	0.60	Standard Proctor	1.3	7.0	2.4
17%	107.4	81%	0.56	Standard Proctor	1.1	3.2	2.5
19%	100.5	76%	0.66	Standard Proctor	0.66	0.0	2.7
19%	101.3	77%	0.65	Standard Proctor	0.84	2.5	2.6
19%	101.7	78%	0.64	Standard Proctor	3.8	2.6	2.0

Data Sets that support the final report

Share Drive folder name and path where data are stored:

\\Bor\do\TSC\Jobs\DO_NonFeature\Science and Technology\2014-PRG-Cracked Embankment Erosion

Point of Contact name, email and phone:

Peter Irey, pirey@usbr.gov, 303-445-3033

Short description of the data:

Photos, videos, calculations, drawings, and reports all documenting the crack embankment erosion research. Research started in FY15 and was completed in FY19, final report was completed in FY20.

Keywords:

CEET, CEET, Erosion, Crack Embankment Erosion Test

Approximate total size of all files:

1,744 Files, 159 Folder, Total Size: 41.6 GB

